NAVAL POSTGRADUATE SCHOOL
Monterey, California

THESIS

GLOBAL SCALE ESTIMATES OF AEROSOL PARTICLE CHARACTERISTICS

by

Edmond M. Frost

December 1988

Thesis Advisor P.A. Durkee

Approved for public release; distribution is unlimited.

Unclassified

security classification of this page

ADA204786

REPORT DOCUMENTATION PAGE

1a Report Security Classification: Unclassified		1b Restrictive Markings	
2a Security Classification Authority		3 Distribution Availability of Report: Approved for public release; distribution is unlimited.	
2b Declassification Downgrading Schedule			
4 Performing Organization Report Number(s)		5 Monitoring Organization Report Number(s)	
6a Name of Performing Organization: Naval Postgraduate School	6b Office Symbol (if applicable): 35	7a Name of Monitoring Organization: Naval Postgraduate School	
6c Address (city, state, and ZIP code): Monterey, CA 93943-5000		7b Address (city, state, and ZIP code): Monterey, CA 93943-5000	
8a Name of Funding Sponsoring Organization	8b Office Symbol (if applicable)	9 Procurement Instrument Identification Number	
8c Address (city, state, and ZIP code)		10 Source of Funding Numbers	
		Program Element No	Project No / Task No / Work Unit Accession No

11 Title (include security classification): GLOBAL SCALE ESTIMATES OF AEROSOL PARTICLE CHARACTERISTICS

12 Personal Author(s): Edmond M. Frost

13a Type of Report	13b Time Covered	14 Date of Report (year, month, day)	15 Page Count
Master's Thesis	From To	December 1988	53

16 Supplementary Notation: The views expressed in this thesis are those of the author and do not reflect the official policy or position of the Department of Defense or the U.S. Government.

17 Cosati Codes			18 Subject Terms (continue on reverse if necessary and identify by block number)
Field	Group	Subgroup	Satellites, Remote Sensing, Aerosols, Optical Depth, Pacific
			Advanced Very High Resolution Radiometer

19 Abstract (continue on reverse if necessary and identify by block number)

NOAA-7 (AVHRR) data from April 1982 and 1983 were used to perform a global scale analysis of aerosol particle characteristics. Several improvements were incorporated into an AVHRR multichannel satellite data technique developed by Pfeil (1986). This included better cloud and sunglint discrimination, removal of Rayleigh radiance and accounting for ozone absorption. The characersitics analyzed were optical depth and Aerosol Particle Size Index (S_{12}). S_{12} provides the slope of the aerosol particle size distribution curve. Both of these parameters were evaluated during several naturally occurring events, foremost of which were the 1982 El Chicon eruption and the 1982-1983 El Nino-Southern Oscillation event. The results provided evidence that a significant amount of aerosol particles over marine regions are from land-derived sources. However, the results also provided evidence that some marine aerosol particles may be of biogenic origins.

Remote Sensing

20 Distribution Availability of Abstract	21 Abstract Security Classification	
☒ unclassified unlimited ☐ same as report ☐ DTIC users	Unclassified	
22a Name of Responsible Individual: P.A. Durkee	22b Telephone (include Area code): (408) 646-3465	22c Office Symbol: 64DE

DD FORM 1473,84 MAR — 83 APR edition may be used until exhausted; All other editions are obsolete

security classification of this page

Unclassified

Approved for public release; distribution is unlimited.

Global Scale Estimates of Aerosol Particle Characteristics

by

Edmond M. Frost
Lieutenant, United States Navy
B.A., Dowling College, 1976
M.S., Long Island University, 1979

Submitted in partial fulfillment of the
requirements for the degree of

MASTER OF SCIENCE IN METEOROLOGY AND OCEANOGRPHY

from the

NAVAL POSTGRADUATE SCHOOL
December 1988

Author: 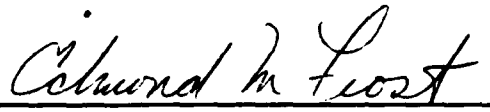

Edmond M. Frost

Approved by: 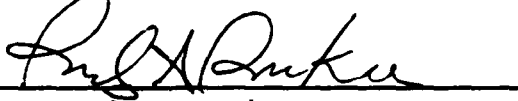

Philip A. Durkee, Thesis Advisor

Carlyle H. Wash, Second Reader

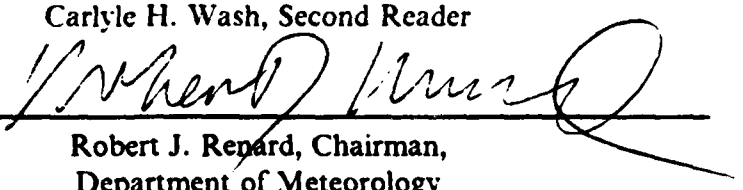

Robert J. Renard, Chairman,
Department of Meteorology

Gordon E. Schacher,
Dean of Science and Engineering

ABSTRACT

NOAA-7 AVHRR data from April 1982 and 1983 were used to perform a global scale analysis of aerosol particle characteristics. Several improvements were incorporated into an AVHRR multichannel satellite data technique developed by Pfeil (1986). This included better cloud and sunglint discrimination, removal of Rayleigh radiance and accounting for ozone absorption. The charactersitics analyzed were optical depth and Aerosol Particle Size Index (S_{12}). S_{12} provides the slope of the aerosol particle size distribution curve. Both of these parameters were evaluated during several naturally occurring events, foremost of which were the 1982 El Chicon eruption and the 1982-1983 El Nino-Southern Oscillation event. The results provided evidence that a significant amount of aerosol particles over marine regions are from land-derived sources. However, the results also provided evidence that some marine aerosol particles may be of biogenic origins.

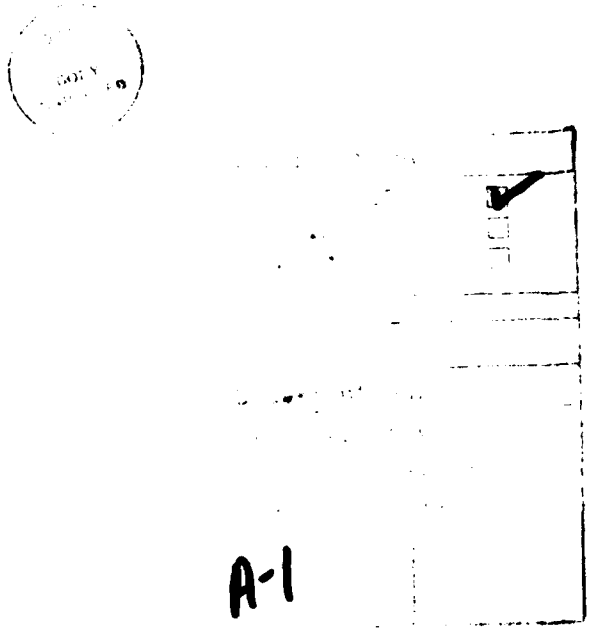

TABLE OF CONTENTS

LIST OF TABLES

LIST OF FIGURES

I. INTRODUCTION

It has been popular to blame weather patterns and their changes on a wide range of events. Some of these events are ridiculous, such as blaming floods on man's first landing on the moon, while others merit serious attention, such as an El Nino-Southern Oscillation and it's effect upon global weather patterns. One source that has received serious attention in the last two decades is the effect that aerosol particles are having on the global climate.

In the middle 1960's, McCormick and Ludwig (1967) hypothesized that a buildup of anthropogenic atmospheric aerosol particles could increase the albedo, thus causing a long term cooling of the earth. Charlson and Pilat (1969) described how aerosol particles affect the energy absorbed by the earth-atmosphere system. In succeeding years, mounting evidence has indicated that atmospheric aerosol particles play a crucial role in the earth's environment.

These particles have the potential to directly influence the earth's heat budget through absorption, scattering and emission of radiation. Atmospheric particles also have a role in atmospheric chemistry. They provide a direct effect through chemical interactions with other atmospheric constituents, such as hydrogen sulfide, and by decreasing incident solar radiation that affects minor constituents such as ozone. Thus, aerosol particles can have a profound effect upon global ecology.

Coakley (1976) presented a model of the earth's radiation budget that inferred a need for spatial distributions of aerosol particles. Meanwhile, Weiss et al. (1976) used a model by Chylek and Coakley (1974) in which actual aerosol particle measurements were compared with clear air assumptions. This clearly demonstrated a need for aerosol particle information within radiation budget models. Short term temporal changes in temperature were linked to changes in aerosol particles during a Soviet investigation of longwave radiation in the tropical Atlantic ocean (Zaitseva, 1976). They observed a 0.3 to 0.4°C/day radiative cooling with haze from North Africa.

In remote marine regions, far removed from continental influences, aerosol particles had been thought to be composed primarily of sea salts. Woodcock (1952 and 1953) measured sea salts in the marine boundary layer and proposed that they were responsible for most of the cloud condensation nuclei in marine regions. Meinert and Winchester (1977) found that the distribution of aerosol particles over the ocean was bimodal and

postulated that this bimodality was caused by large marine particles (sea salts, supermicron size) and continental particles (land originated, submicron size). The collective work of Carlson and Prospero on Saharan dust during the 1970's documents the invasiveness of continental particles over marine regions (Carlson and Prospero, 1972; Prospero and Nees, 1976; Carlson, 1978; Prospero, 1982).

Patterson et al. (1980) measured a clearly bimodal distribution in remote regions during Global Atmospheric Measurements Experiment of Troposheric Aerosols and Gasses (GAMETAG) flights. He postulated that the smaller sized particles were marine in origin, not continental. Direct observations made by USNS LYNCH and NOAA ship DISCOVERY in 1983 and 1984 (Hoppel et al., 1987) revealed peaks at 0.02μm and 0.08 to 1.5μm. The samples taken during these cruises revealed that the aerosol particles were totally marine in origin and that the particles were too volatile to be predominantly sea salts. Hoppel et al. (1987) has demonstrated a method whereby both peaks could be produced by a stepwise process that starts with Dimethylsulfide (DMS) and ends with sulfur based cloud condensation nuclei (CCN)

Hoppel et al. (1987) produced the bimodal distribution by converting DMS, through photooxidation into a product of low volatility, methyl sulfonic acid (MSA). MSA forms particles through homogeneous nucleation. Condensation of MSA and water produces a surface area size increase. Condensation starts when the MSA particles reach a radius of 0.04μm. This was considered by Hoppel et al. (1987) as a threshold radius for cloud activation. The conversion of DMS to MSA cloud condensation nuclei is a rapid process, usually taking less than 12 hours. In a bimodal distribution, nucleation forms the smaller size distribution while condensation resulted in the large peak. Fig. 1, from Hoppel et al. (1987), shows how DMS initiated aerosol particles can increase in size over a period of time to form CCN.

Much of the early evidence for oceanic sulfur sources tried to show a link between the ocean and atmosphere through fluxes of biogenic hydrogen sulfide and sea salt sulfates (Kellog et al., 1972). Lovelock et al. (1972) was the first to postulate DMS as the prime oceanic sulfur source. Since then, more evidenced from Charlson et al. (1987) gives credence to Lovelock's original hypothesis. DMS also has been found to be strongly linked to algal productivity in a variety of settings and in tropical regions in particular (Andrea, 1985). Regardless of the source, oceanic sulfur is now postulated to contribute 30% of the atmosphere's sulfur.

If oceanic sulfur does contribute significantly to the atmospheric sulfur budget, then oceanic changes affecting that sulfur source would indirectly alter the earth's heat budget

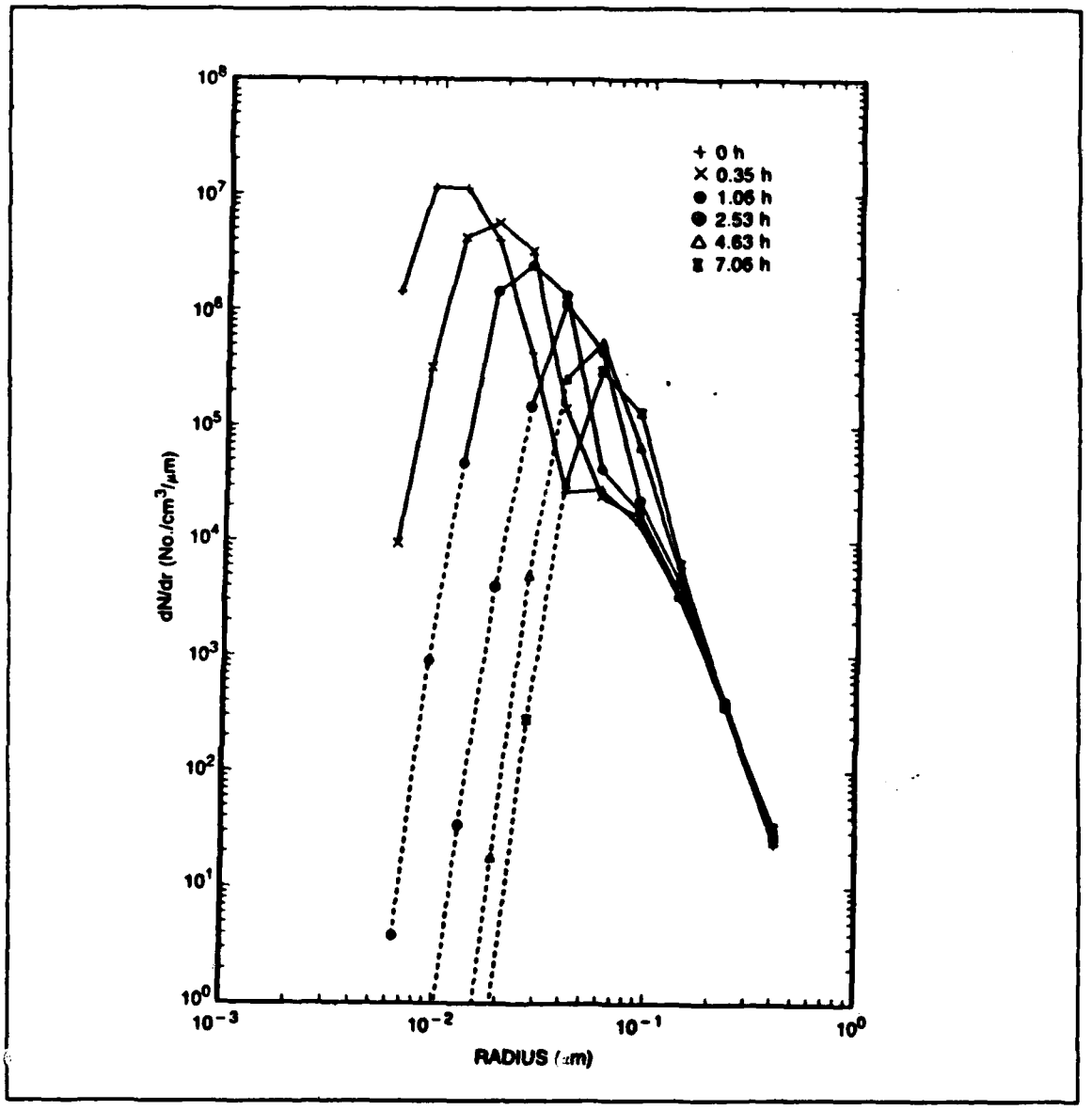

Fig. 1. Observed evolution of particle-size distribution of DMS irradiation, from Hoppel et al. (1987).

through the production or nonproduction of sulfur-based aerosol particles. Charlson et al. (1987) proposed a biological feedback mechanism for the earth's radiation budget, illustrated in Fig. 2, that uses sulfur-based aerosol particles as the buffer.

Almost the entire body of knowledge of aerosol particles over the ocean has come from direct observations by ships or aircraft. While providing excellent data, the area

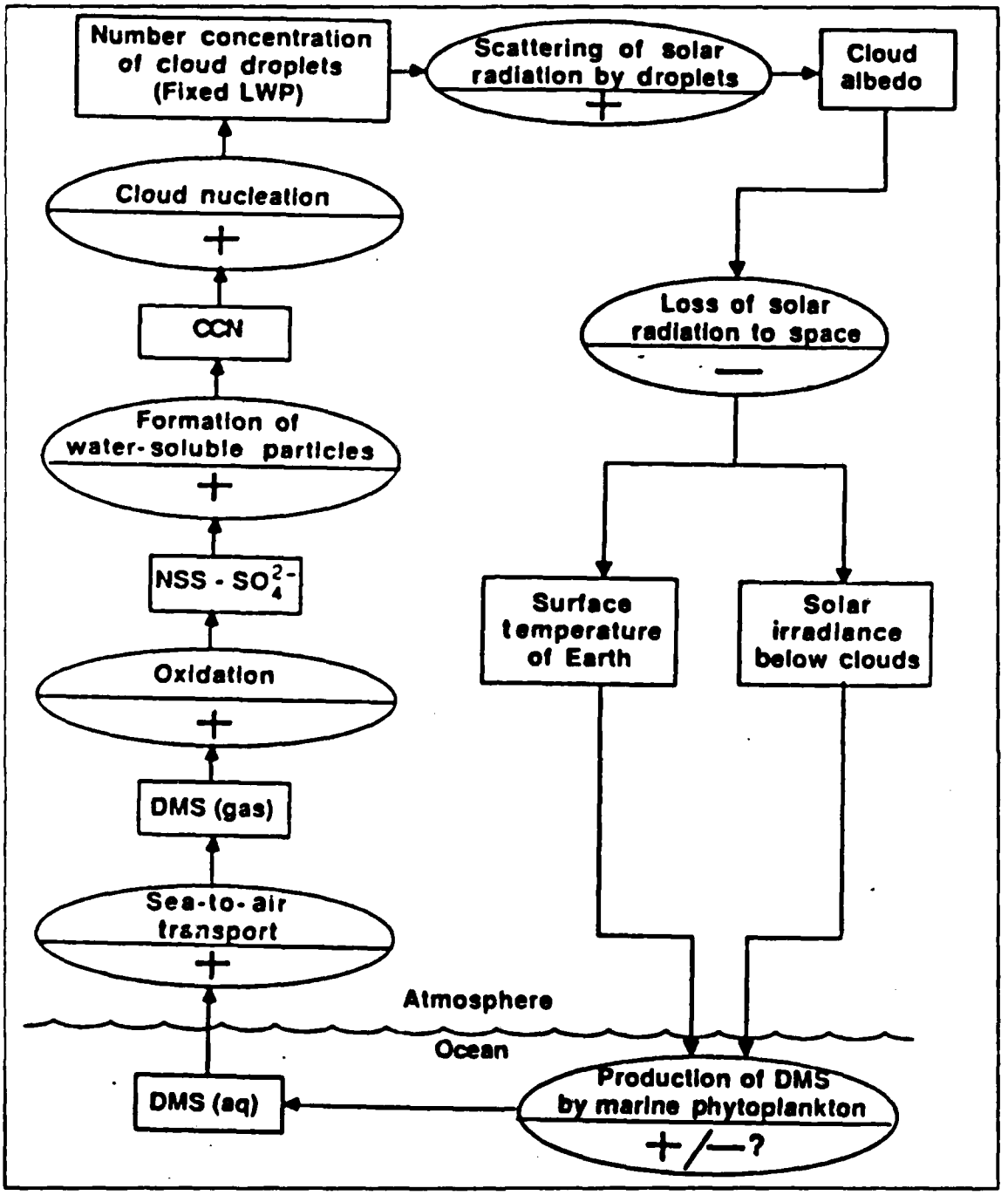

Fig. 2. Biological feedback in the earth's radiation budget, from Charlson et al. (1987).

covered is limited. Also, this method of data collection does not provide for long term continuous coverage of a specific location nor does it give broad coverage of an ocean basin.

Presently, the only method of continuously monitoring aerosol particles on a global scale is by satellite remote sensing. While unable to detect the type of aerosol particle, satellites measurements can infer the relative size (large or small) of marine aerosol particles in a given volume of air. When correlated with other occasional in situ data sources, such as cruise data, they can give a good measuremnent of the spatial and temporal distribution of atmospheric particles. Satellite measurements of aerosol particles made on a global scale can provide a better understanding of the complex interrelationship between the atmosphere and the ocean.

The major purpose of this research is to develop a global scale perspective of aerosol particles and their role in the earths environment. In this thesis, multi-channel satellite data are used to measure global scale patterns of aerosol particle characteristics. Improvements in sunglint and cloud discrimination are incorporated into the procedure and the results are compared with the similar work done by Pfeil (1986) on the same data set. Pfeil (1986) used the satellite-measured red and near infrared radiance to infer the size relationship of aerosol particles. This was accomplished by forming a ratio of the albedos, as determined from those two wavelenghts.

Additionally, an improvement in optical depth determination over the oceans is explored using a variable scattering phase function. A result of Pfeil's work is that marine aerosols are not uniform in size or composition. Therefore, a single, constant scattering phase function is inadequate to accurately describe the spectral scattering by aerosol particles.

Finally, the beginnings of an interannual comparison is performed through analyzing data sets for the same month in two years. The data sets are from before and during the 1982-1983 El Nino-Southern Oscillation (ENSO) event. This thesis will show that variations in aerosol particle characteristics are observable during an event of the magnitude of an ENSO.

II. THEORY

Aerosol particles are remotely-sensed by satellites through their interactions with various wavelengths of upwelled radiation. This interaction can be by absorption, emission or scattering. For the purposes of this discussion, only red visible and near infrared wavelengths will be used. The reason for this limitation will be discussed below.

There are three primary sources of upwelled radiation in cloud-free areas, scattering by molecules in the atmosphere, scattering by larger particles called aerosols and the earth's surface. In the red and near infrared wavelengths, aerosol particles are the dominant scatterer over the ocean. Except for sunglint, reflectance by the ocean is very small and scattering by molecules does not vary spatially.

Satellites detect the upward scattered radiation from aerosols particles as upwelled radiance. Durkee et al. (1986) showed that there is a direct correlation between the upwelled radiance measured at the satellite and aerosol particle optical depth. Since optical depth is linked to the size and distribution of aerosol particles it should be possible to relate the satellite detected radiance to the size distribution of marine aerosols. While it has not been possible to develop a satellite technique for directly obtaining an aerosol particle size distribution, Bullfinch (1986) developd an approach for infering the size of aerosol particles. He used variations in radiance detected at red and near infrared wavelengths for an aerosol particle as an indicator of it's size. This process can best be explained by understanding the processes involved in the radiant energy transfer through the atmosphere.

A. RADIATIVE TRANSFER IN THE MARINE ATMOSPHERE.

Liou (1980) gives the following as the radiative transfer equation (refered to hereafter as RTE) for solar radiation in a plane parallel atmosphere.

$$\mu \mathrm{d}L(0;\mu,\phi)/\mathrm{d}\delta = L(\delta,\Omega) - (\omega_0/4\pi)\int_{4\pi} L(\delta,\Omega')p(\Omega,\Omega')\mathrm{d}\Omega' - (\omega_0/4\pi)\pi F_0 p(\Omega,-\Omega_0)e^{(-\delta/\mu_0)}, \tag{1}$$

where

L = diffuse radiance,

δ = optical depth,

ω_0 = single scattering albedo,

$\mu = \cos\theta$ ($\cos\theta$ = satellite zenith angle),

$\mu_0 = \cos\theta_0$ (θ_0 = solar zenith angle),

Ω = solid angle(θ,ϕ) (ϕ = azimuth angle),

$p(\Omega, \Omega_0)$ = scattering phase function and

πF_0 = incoming solar radiative flux.

The first term on the right hand side of the equation accounts for attenuation through either scattering or absorption. The second term describes the intensity added to the beam by multiple scattering. The third term accounts for single scattering intensification. For a more complete discussion, see Liou (1980).

Over the ocean the RTE can be simplified due to the radiative properties of maritime air. Whenever the optical depth is small, the average path length between particles is relatively large. In general, optical depth over the ocean is less then 0.2 (Pfeil, 1986). If the aerosol particles are assumed to be randomly distributed and there is relatively large distance between them, single scattering dominates over multiple scattering. Therefore, it is reasonable to assume that the multiple scattering term of equation (1) is very small and can be disregarded. At these wavelengths the upward radiated intensity from the surface is also small (Sellers, 1965). Thus the RTE, reduces to

$$L(0; \mu, \phi) = (\omega_0 \mu_0 F_0 / 4(\mu + \mu_0)) p(\Theta)(1 - e^{(\delta(1/\mu + 1/\mu_0))}). \tag{2}$$

For an optically thin atmosphere, $\delta(1/\mu + 1/\mu_0) << 1$. Therefore, the RTE can be further simplified to

$$L(0; \mu; \phi) \sim (\omega_0 F_0 / 4\mu) p(\Theta)\delta, \tag{3}$$

where Θ is the single scattering angle.

B. OPTICAL DEPTH

Optical depth provides a measure of the mass of absorbing and emitting material in an air column. It is defined as

$$\delta = \int_0^H \beta_{ext} dz, \tag{4}$$

which is the extinction coefficient of the atmosphere integrated from the surface to the

height of the satellite. This is the total extinction of the atmosphere. The extinction coefficient is given by

$$\beta_{ext} = \int_0^\infty \pi r^2 Q(m,r)_{ext} n(r) dr, \tag{5}$$

where πr^2 is the cross sectional area of the particle and n(r)dr is the size distribution of the particles at that cross sectional area. Q_{ext} is an extinction efficiency factor that varies with the radius (r) and composition, through the index of refraction (m).

These equations show the relationship between optical depth and the aerosol particle. β_{ext} is a function of the aerosol particle size and distribution. Since optical depth is a function of β_{ext}, it follows that changes in the aerosol particle size or distribution will be reflected in optical depth.

Attendent with these changes in the aerosol particles is a change in the radiative properties of the atmosphere. Equation (3) shows that any change in the optical depth results in a change in the diffuse radiance that leaves the atmosphere. These changes are not only important in the measurement of atmospheric properties, but they also produce effects that are widely felt by other users of the electro-optical spectrum.

In addition to detected radiance, optical depth is a function of single scattering albedo (ω_0), satellite zenith angle (μ), solar radiation (F_0) and scattering phase function ($p(\Theta)$). Based upon earlier assumptions, the major variables in determining optical depth are satellite zenith angle and phase function. Durkee (1984) showed that satellite zenith angle is the most critical factor effecting the radiance-optical depth relationship. Phase function was determined to play only a small role.

Phase function only plays a small role if the aerosol particles in a given volume of air have a constant size distribution. This is a good assumption to make for small scale analyses. It is a poor assumption for large scale or global scale analysis, where large changes in the aerosol particle size distribution would be expected. When the aerosol size distribution changes, the phase function must change also. Fig. 3 illustrates how phase function can change with relative humidity. On a global scale analysis, changes in ambient relative humidity must be expected. Therefore, any large scale analysis, utilizing a constant phase function produces a significant error. A more accurate representation, albeit more difficult, is to calculate optical depth with a phase function that varies with the dominant aerosol particle.

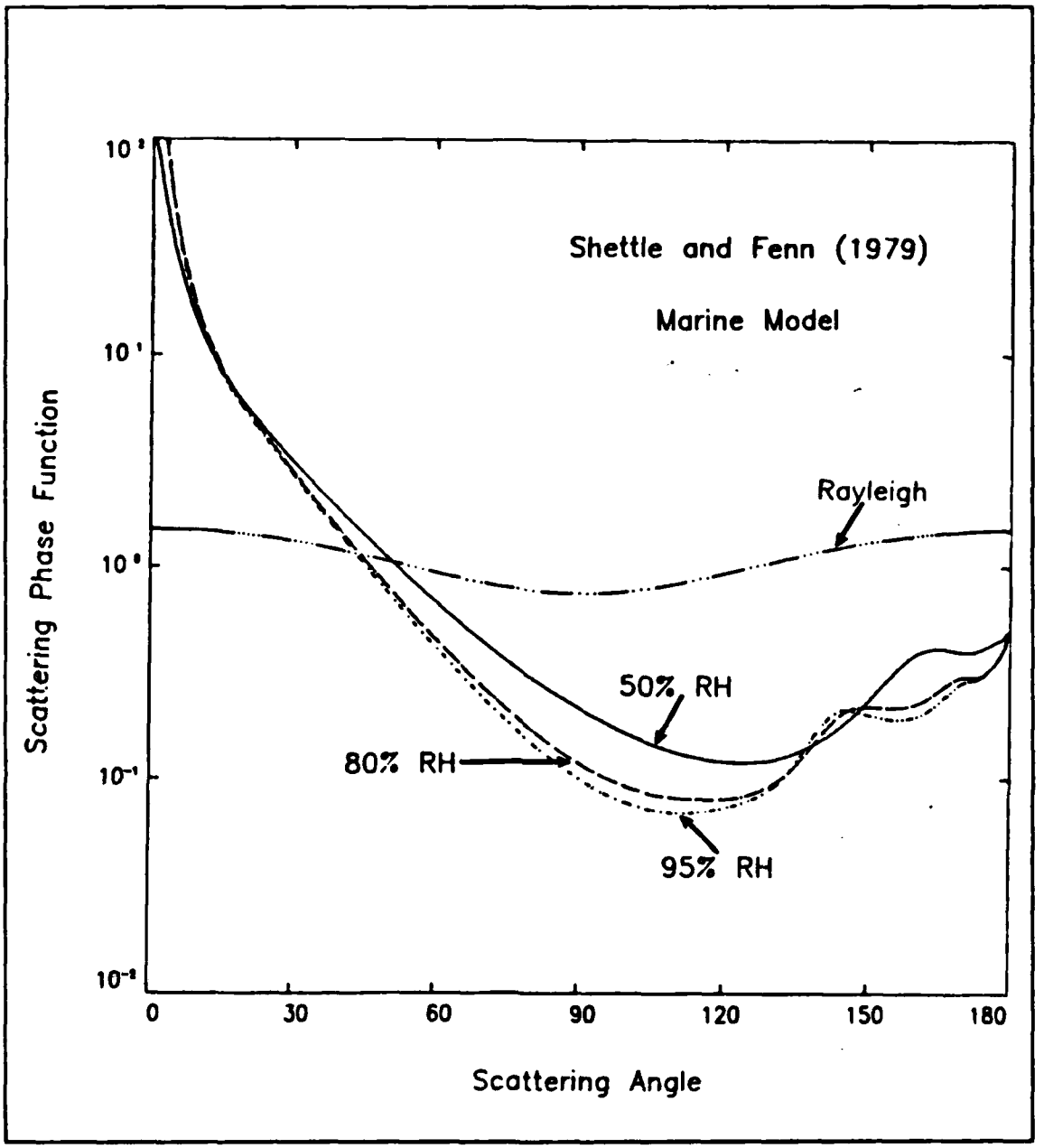

Fig. 3. Marine phase functions (after Shettle and Fenn, 1979)

C. AEROSOL OPTICAL DEPTH

The satellite detected radiance from equation (3) is the sum of aerosol particle radiance and path-added Rayleigh radiance ($L = L_A + L_R$). Path-added Rayleigh radiance is radiant energy that is due to Rayleigh scattering in the atmosphere. Rayleigh scattering

occurs when the wavelength of the radiation is much greater than the size of the scattering material. At red and infrared wavelengths, the scattering material is primarily due to atmospheric molecules. The Rayleigh radiance must be accounted for in order to obtain the radiance due strictly to aerosol particles. By subtracting the Rayleigh radiance, equation (3) then becomes

$$L_A = L(0; \mu; \phi) - L_R \sim (\omega_0 F_0/4\mu) p(\Theta) \delta_A, \tag{6}$$

where δ_A is aerosol particle optical depth.

It is possible to express the optical depth of the atmosphere as a function of measured diffuse radiance by solving for

$$\delta_A \sim (4\mu/\omega_0 F_0) p(\Theta) L_A. \tag{7}$$

This equation provides an understanding of the radiative properties of the atmosphere and, as will be seen, an insight into the size and distribution of atmospheric aerosol particles.

D. RADIANCE AND AEROSOL SIZE DISTRIBUTION

It has been determined that the aerosol particle dependent terms in the RTE are larger at red wavelengths than at near-infrared wavelengths for small aerosol particles (Durkee, 1984). Since the diffuse radiance is proportional to aerosol particle dependent terms, spectral variations in radiance result from variations in the aerosol particle dependent terms. The spectral variation can be quantified by a simple ratio between red wavelengths and near-infrared wavelengths. This results in

$$\frac{(L_A)_{red}}{(L_A)_{nir}} \sim \frac{(\omega_0 F_0/4\mu) p(\Theta) (\delta_A)_{red}}{(\omega_0 F_0/4\mu) p(\Theta) (\delta_A)_{nir}}. \tag{8}$$

Since for small aerosol particles, the aerosol particle dependent terms are larger, the ratio will be larger when smaller aerosol particles dominate in an area.

Earlier it was noted that there was a linear relationship between aerosol particle optical depth and satellite detected radiance. This relationship is shown in Fig. 4. This relationship is linear because ω_0 is approximately one at red and near infrared wavelengths and $P(\Theta)$ changes are small with wavelength variation (Durkee, 1984). F_0 varies

as a function of wavelength, but this only results in a proportionality constant. The value of μ is the satellite view zenith angle, which does not change with wavelength. The ratio, called the Aerosol Particle Size Index (S_{12}), can now be simplified to

$$S_{12} = \frac{(L_A)_{red}}{(L_A)_{nir}} \approx \frac{(\delta_A)_{red}}{(\delta_A)_{nir}}, \tag{9}$$

where δ_A is optical depth due to aerosol particles.

Satellite derived measurements cannot provide the actual aerosol particle size distribution curve, but the ratio described above does give the slope of that distribution curve. The steeper, the slope the greater the influence of small particles on the distribution and vice versa.

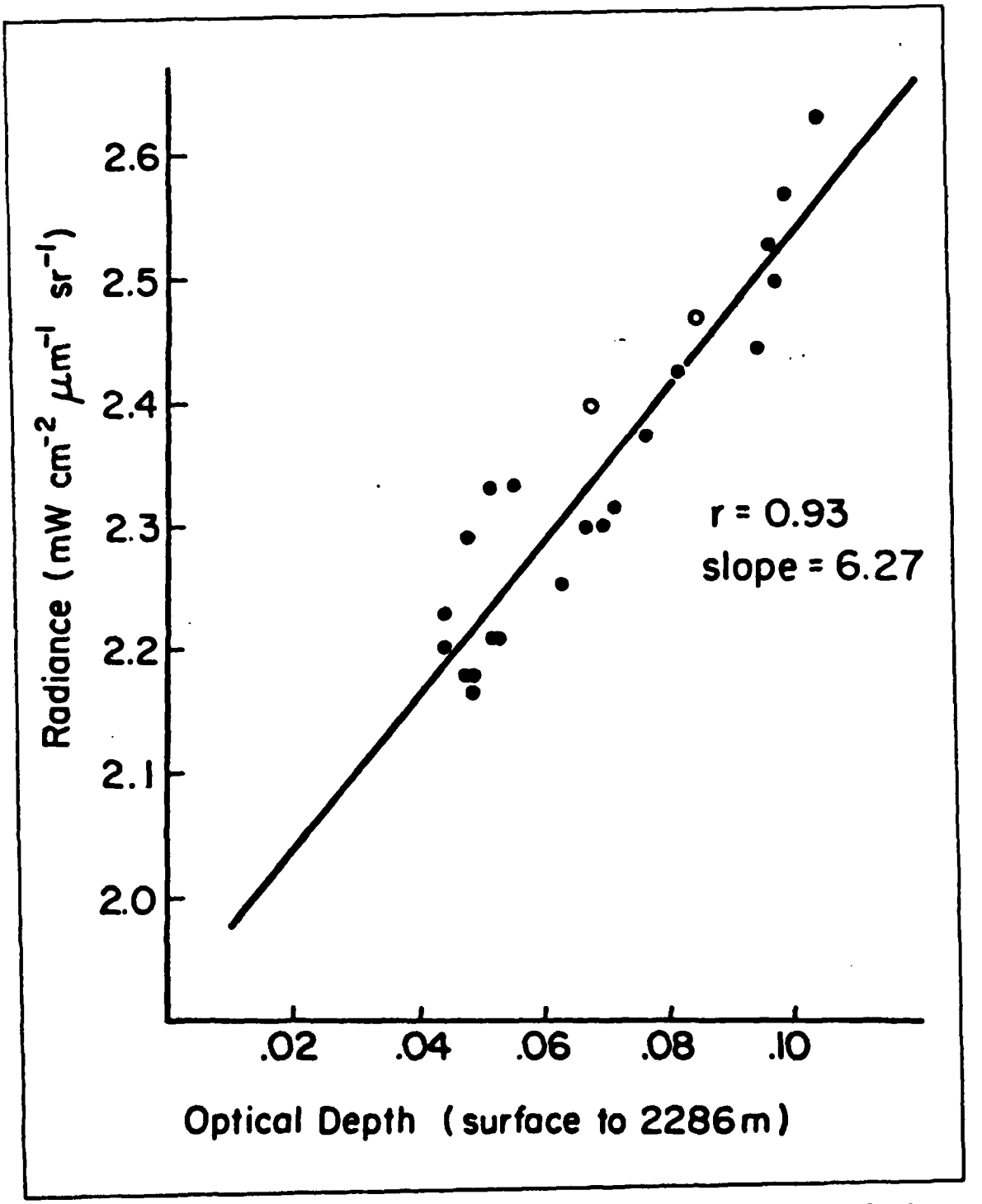

Fig. 4. Satellite detected radiance vs. aircraft measured optical depth, from Durkee (1984).

III. PROCEDURES

A. DATA

The data were collected by NOAA-7, a sun-synchronous polar orbiting satellite with an average altitude of 833 km. It's equator crossing time is approximately 0230 local standard time northbound and 1430 local standard time southbound. Upwelled radiance was measured by the Advanced Very High Resolution Radiometer (AVHRR) in five spectral bands or channels. Table 1 provides the bandwidths of these channels. Channels 1, 2, 3 and 4 are used in this study.

Table 1. NOAA 7 ADVANCED VERY HIGH RESOLUTION RADIOMETER CHANNEL BANDWIDTHS, AFTER JENSEN (1986).

Channel	Bandwidth	Radiance
1	0.58-0.68μm	Red Visible
2	0.725-1.10μm	Red Visible Near Infrared
3	3.55-3.93μm	Mid Infrared
4	10.5-11.3μm	Thermal Infrared
5	11.5-12.5μm	Thermal Infrared

The source of AVHRR data was a multi-year archive maintained at the National Center for Atmospheric Research (NCAR), Boulder, CO. From the AVHRR data for April 1982, two six-day periods, 5-10 April and 20-25 April, were studied. The area covered in this subset was the North and South Pacific Oceans, from 50°N to 50°S and from 110°E to 70°W. In addition, AVHRR data for April 1983 were also processed from the NCAR archives. The April 1983 data provided full global coverage. These data were for the full month, but only the odd numbered days of the month were studied. April 1982 data were analyzed in the two time periods, the 5th-10th and the 20th-25th, to provide a direct comparison with the work done earlier by Pfiel (1986).

B. DATA PROCESSING

The April 1982 data were processed at the Interactive Environmental Digital Analysis Laboratory (IDEA LAB) located at the Naval Postgraduate School (NPS), Monterey, CA. The heart of this lab is a VAX 8250 computer, with graphics display terminals. The April 1982 data, which were global data set, was processed on NCAR's

Cray XMP supercomputer with the assistance of the NCAR Scientific Computing Division. The April 1982 data were digitally transmited to the NPS IDEA LAB when processing was completed.

The IDEA LAB was used to produce visual images from the processed data. The ability to enhance these images while working at the IDEA LAB's work stations facilitated the interpretation and analysis of the images.

C. DATA ANALYSIS

The data analysis scheme was based on that used by Pfiel (1986), with several improvements. Additionally, several other atmospheric features were analyzed, extending the early work. The final processing produced the following data sets:

Channel 1 Channel 2 radiance ratios.

Optical depth using a marine phase function.

Optical depth using a rural phase function.

Optical depth using a variable Heney-Greenstien phase function.

Channel 1 reflectance for low clouds.

Channel 3 reflectance for low clouds.

Number of partly cloudy pixels.

Number of high cloud pixels.

All of the results were stored and averaged in 1° by 1° boxes. The number of AVHRR pixels stored in each box varied, depending upon a series of pixel tests. Although cloud data were calculated, it was not evaluated as part of this thesis. When the final images were produced, each data point is one of these 1° by 1° boxes.

In Pfiel (1986), sunglint was removed by eliminating the entire western half of each image from 40°N to 10°S. This approach was overly conservative. While it ensured that there would not be any contamination due to sunglint, it also removed data points that were not contaminated. Since sunglint is a function of viewing geometry, it is feasible to remove it more carefully by calculating an elliptical-shaped area. This is smaller than the rectangle used in the earlier work. This approach added about 25% of the removed area back into processing, but still provided assurance that little or no sunglint contamination occurred.

Cloud removal was changed to a purely objective analysis vice a subjective/objective analysis used by Pfeil. All the image pixels were subjected to the following tests in the order listed below:

1. Test for bad pixels: If channel 2 or channel 4 radiance values are less then zero, after Rayleigh radiance was removed, then the pixel is classifed as "bad" and not processed.
2. Test for high clouds: A pixel was considered to contain high clouds if it's channel 4 brightness temperature was less then 273°K.
3. Test for low clouds: A pixel was considered to contain low clouds if it's channel 2 albedo was greater then 40%.
4. Preliminary test for clear pixels: A channel 1/channel 2 albedo ratio was calculated and if that ratio was greater then 1.5 the pixel was tentatively classified as clear.
5. Final test for clear pixel: The channel 2 albedo of the pixel tentatively identified as clear was compared with the four pixels above, below, to the right and to the left. All the pixels must fall with in five counts of each other for the pixel to be classified as clear, otherwise it was counted as partly cloudy. A count is equivalent to 0.1069% albedo.

Equation (3) expresses a relationship for the measured radiance in both channels 1 and 2 over the ocean. In Pfiel's earlier work, total radiance was assumed to be dominated by aerosol particle scattering, therefore Rayleigh radiance need not be accounted for. However, this is not the case for optical depth.

Preliminary tests indicated a large difference in optical depth for cases with and without Rayleigh radiance removed. For cases that included Rayleigh radiance, optical depth estimates averaged 0.22 higher than in cases where Rayleigh radiance was removed. This is a significant value since the highest optical depth estimate obtained was 0.82. The cases including Rayleigh radiance showed optical depth ranges from 0.18 to 0.82. Optical depth in the cases where Rayleigh radiance was removed ranged from 0.06 to 0.54 with an average value of 0.24. For this reason, path-added Rayleigh radiance was removed.

The removal of the Rayleigh radiance also produced another change in the procedure. Previously, the ratios were calculated using the albedo from each channel, rather than the radiance. This choice was made based on computational considerations. To remove the Rayleigh radiance also requires the determination of the ratios using radiances.

A total of three optical depth calculations were performed using three separate phase functions. As discussed earlier, due to the changing nature of aerosol particles over various oceanic regions, any one invariant scattering phase function was felt to be inadequate. The three phase functions used were a "classical" marine phase function (Shettle and Fenn, 1979), a continental rural type phase function modified for over ocean usage and a varying phase function.

The two constant phase functions were used to determine whether accurate results were obtainable using a simple phase function. Optical depths are much easier to derive using a constant phase function. However, the results may not be adequate for a global scale analysis. Using all three phase functions would provide a method of choosing the most appropriate one for global scale estimates of optical depth.

Based upon the considerations just discussed, an appropriate phase function was chosen. Fig. 5 shows a composite of optical depths taken from several successive satellite passes in a single day (5 April 1982). From this figure it can be clearly seen that the optical depth estimate that included the constant marine phase function (Shettle and Fenn, 1979) was inconsistent. The optical depths varied across the width of the satellite pass, from west to east, with a maximum in optical depth towards the west side, decreasing towards the east. In contrast, optical depths are more uniform when a varying single scattering phase function is used. The optical depths are fairly uniform across the width of the passes and the overall optical depth results were in the expected range of less then 0.25. The optical depths from the invariant phase function were much higher than expected, with large areas having values above 0.5.

A problem with using an invariant phase function is that it is based upon a volume of air containing a uniform aerosol particle size distribution. Any significant deviation from that aerosol particle size range and the scattering angles predicted by that phase function will be erroneous. A major premise of this work, based on the results of Pfeil (1986), is that the aerosol particles over the ocean are not uniform in size or distribution. It is obvious , from the small sample shown in Fig. 5, that the constant phase function is resulting in optical depths that are too high, greater than 0.5, (ie., greater than 0.5), on the western side of the images.

The relationship between optical depth and phase function was presented in equation (7) from Chapter II. Optical depth, δ_a, is inversely proportional to the $p(\Theta)$. Thus, when the western portion of the satellite images show evidence of optical depths too high, $p(\Theta)$ is too small. Since the overall optical depths are too high , the constant phase function is most likely predicting too much forward scattering for the aerosol particles present. From Mie scattering theory, it can be deduced that the aerosol particles actually present are smaller then the aerosol particles from which the marine phase function was developed.

The variable single scattering phase function is superior because it starts to account for differences in the aerosol size distribution. It works on the basis of choosing the best phase function, based upon an inferred aerosol particle size. By providing the correct

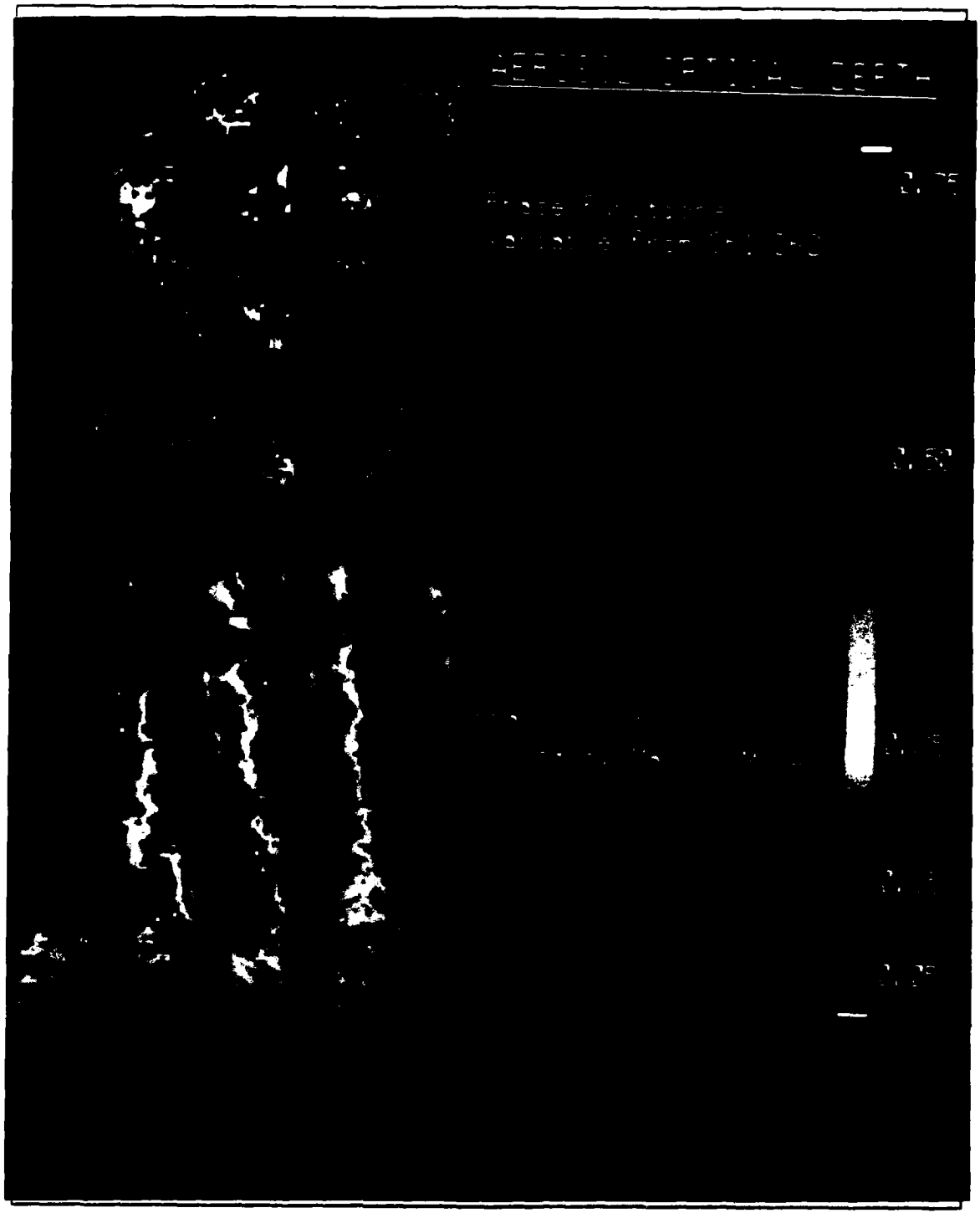

Fig. 5. A comparison of optical depths as determined from an invariant and a variable phase function. (5 April 1982)

phase function for an aerosol particle distribution, a more accurate optical depth estimate is produced.

The relative sizes of the aerosol particles are determined by the S_{12} value and based upon this ratio a phase function is calculated. This provides for a close fit between phase function and aerosol particle size. In Fig. 6, the higher ratios, which are due to smaller aerosol particles, have more backscattering radiance than the lower ratios, which are due to larger aerosol particles. This provides the correct $P(\Theta)$ needed to estimate the optical depths expected from small particles.

The variable phase function used was a two term Heney-Greenstein scattering phase function (Lenoble, 1985).

$$P(\Theta) = \frac{W(1-g_1^2)}{(1+g_1^2-2g_1\cos(\theta))} + \frac{(1-W)(1-g_2^2)}{(1+g_2^2+2g_2\cos(\theta))}, \tag{10}$$

where W is a weighting factor and g_1 and g_2 are assymetry curve factors. All three of these factors are functions of S_{12}:

$$W = 1.2 - (0.25 \times S_{12}), \tag{11}$$

$$g_1 = 1.04 - (0.08333 \times S_{12})\wedge \tag{12}$$

$$g_2 = 1.2 - (0.58333 \times S_{12}). \tag{13}$$

As equations 10-13 show, the phase function varies as a function of S_{12}. The basic assumptions are that in areas that have relatively low ratios, the aerosol particles are large and in areas of high ratios the aerosol particles are small. Larger aerosol particles are assumed to follow a marine type phase function, while the smaller particles are assumed to follow a rural type phase function. As the ratios change, the factors used change, thus varying the phase function from one similar to a marine phase function to one similar to a rural phase function. Fig. 6 shows some of the variable phase functions calculated along with the S_{12} used in the calculations.

One final change in the the procedure is an accounting of the effects of ozone. Ozone is a weak absorptive substance in the red and near-infrared wavelengths. It's absorption is greater in the red visible spectrum than the near infrared. The major absorption is at a wavelength of 0.69μm (Fleagle and Businger, 1980), which is found in channel 1 of the AVHRR. A much smaller amount of radiative absorption occurs in channel 2. This produces an unequal amount of ozone absorption of both incoming and

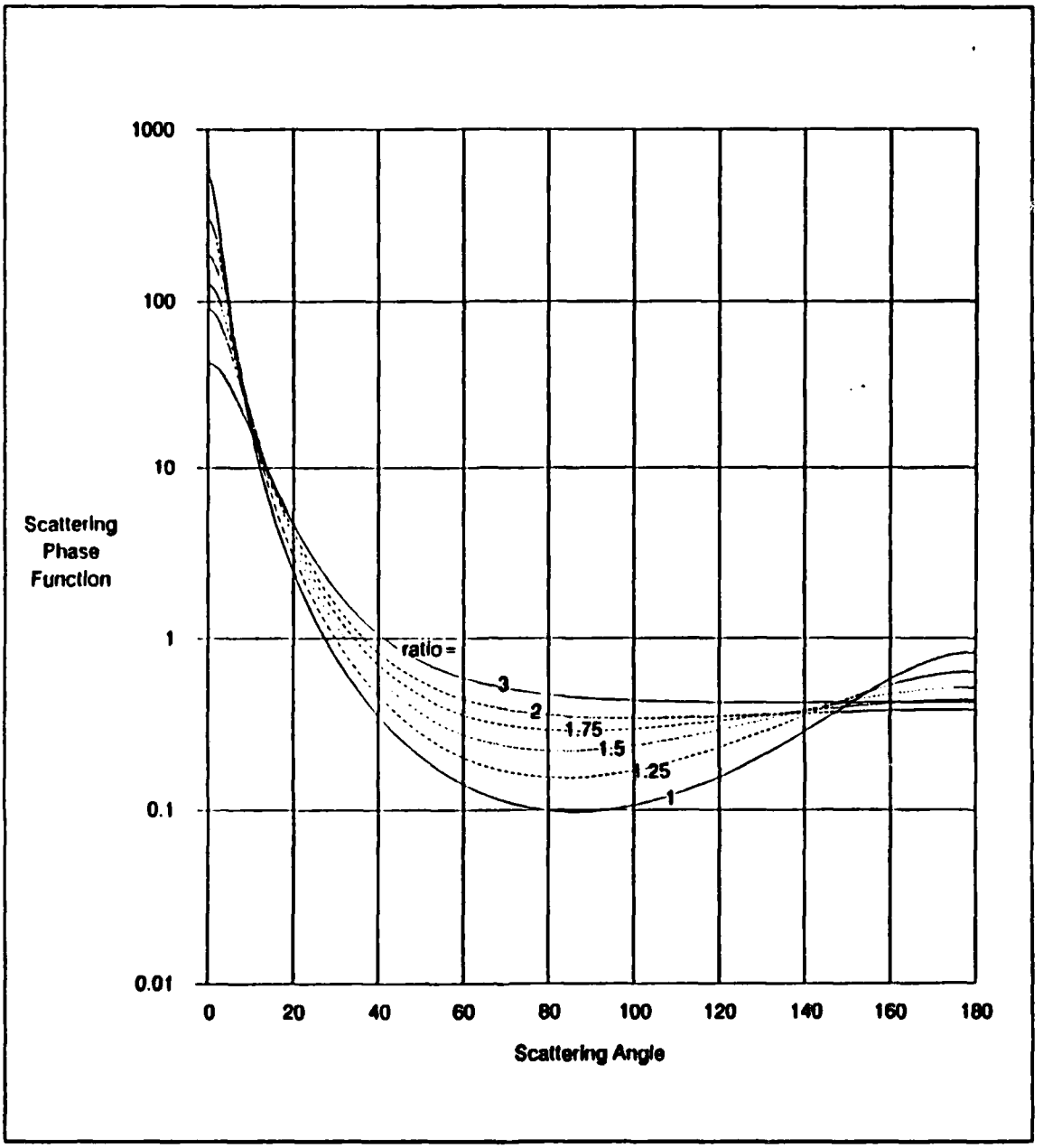

Fig. 6. Aerosol Particle Size Index and associated phase functions.

outgoing radiation. Since the amount of loss due to ozone is a function of wavelength and view zenith angle, it must be properly accounted. Although ozone absorption is the smallest of the changes, it can produce up to a 10% change in estimate of optical depth.

IV. RESULTS AND DISCUSSION

A. AEROSOL PARTICLE SIZE INDEX (CH1/CH2 RATIO) AND OPTICAL DEPTH

1. Intercomparison of Ch1/Ch2 ratio techniques

First, an analysis was performed comparing the current data processing scheme with the results obtained in Pfeil (1986). A direct comparison is only possible in the ratio results, because Pfeil (1986) calculated albedo and did not estimate optical depth.

Fig. 7 and show the S_{12} values from April 1982 for Pfeil's earlier work and the current study. Both results agree in a maximum S_{12} value in the tropics, with the highest values located close or over the equator. They both indicate that the S_{12} values decrease poleward of the tropics, but with a big difference between them in the amount of decrease in the northern hemisphere. Pfeil's results indicate that the decrease in the northern hemisphere is equivalent to the decrease in the southern hemisphere. His calculated S_{12} values ranged from a maximum 2.0 at the equator, decreasing poleward to an average of 1.2 in the midlatitudes. Effectively, the northern hemisphere is equal to the southern hemisphere. The present work does not have equivalent decreases. The average S_{12} in the northern hemisphere for the present study is 1.9, while in the southern hemisphere it is 1.65.

This comparison also indicates that Pfiel's 1986 results underestimate the S_{12} globally. His maximum in the tropics averages 1.8, which is lower than the present work's tropical average of 2.2. Pfeil's S_{12} estimates also are too low in the mid-latitudes, as discussed above.

On a smaller scale, there are differences in the Gulf of Mexico, the northwestern coast of Australia and the southern coast of Australia. Pfiel's study, shows a minimum in S_{12} values in the Gulf of Mexico. In the present work, the values observed in the Gulf of Mexico are much higher, approximately double Pfeil's results. Off the northwestern coast of Australia, Pfiel's work showed some of the highest values observed, greater than 2.0. Also, off the southern coast of Australia is a relative maximum, approximately 1.8. While the S_{12} values observed in both studies for these areas were approximately the same, they are not maximums in the present study.

There are several reasons for these differences. These include the removal of Rayleigh radiance and accounting for ozone absorption in the present scheme along with a better cloud discrimination technique.

Rayleigh radiance removal has a two-fold influence. The first is that it lowers the channel one radiance more than the channel two radiance. This produces a final S_{12} value that is lower than the S_{12} produced with Rayleigh radiance included. Also, the removal of Rayleigh radiance eliminates most of a geometric dependence found in the earlier S_{12} values. In Fig. 7 a strong dependence on geometry is visible, particularly in the late April image. Higher values are observed towards the eastern half of the passes. This is due to the satellite sun-geometry, where the incoming incident solar radiation, because NOAA-7 is an afternoon satellite, is along the western edge of the pass. This produces a maximum in path-added Rayleigh radiance along the eastern portion of the satellite pass, along with a greater amount in channel 1 than in channel 2. This most likely accounts for some of the higher S_{12} values observed in the northern hemisphere, since the solar elevation is higher in the northern hemisphere at this time.

Another contributing factor to the northern hemisphere having lower S_{12} values in the earlier study is that the cloud discrimination technique is not as effective. Clouds, with their large water droplets, would produce low S_{12} values. The blank area in Fig. 8, which is an area that does not contain any clear pixels, has almost a sixfold increase over the blank area in Fig. 7. This extra blank area can be equated to an increase in the ability of the current method to eliminate cloud contaminated pixels. The earlier approach allows a number of cloud contaminated pixels to affect the albedo ratio values.

When the maximum S_{12} values are compared between the two sets of results, it should be noted that the current work produces higher maximum values than Pfeil's study. This is probably due to ozone absorption correction. This absorption varies with wavelength and path angle through the stratospheric ozone layer. The longer near-infrared wavelength is absorbed less then the shorter wavelengths. The result is some elevation of the S_{12} values with an ozone absorption correction.

The differing sunglint removal techniques has two effects. The first effect is that the artificial line that is observable in the tropics in Fig. 7 is no longer visible in the later work (Fig. 8). This line, that was produced previously, was strictly due to a straight east-west line being the northern and southern most limits of the sun glint removal region. The second effect of the sunglint removal technique is to add more useful data pixels into the statistics. This likely accounts for the smoother pattern shown in Fig. 8.

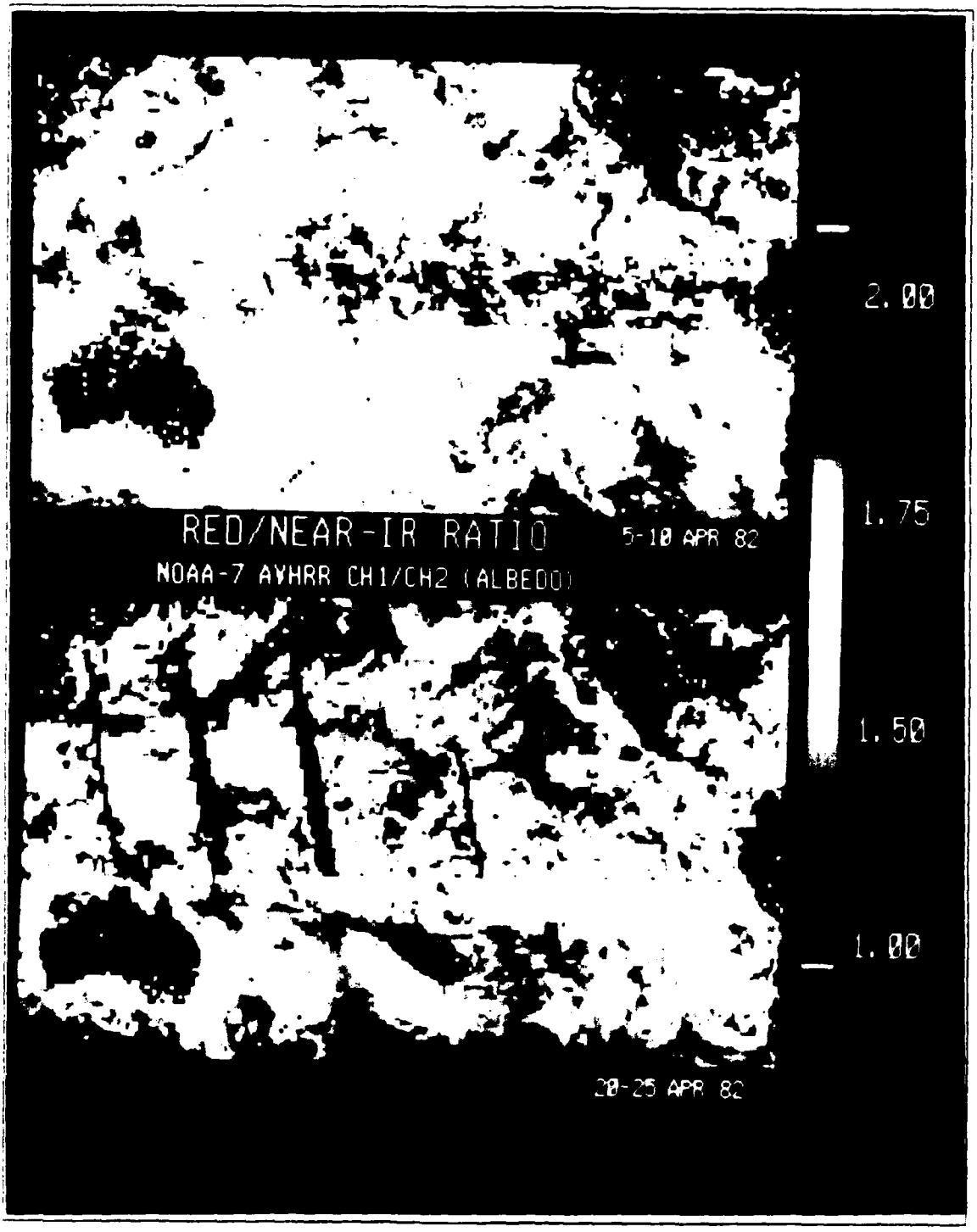

Fig. 7. Aerosol Particle Size Index for early and late April 1982 from Pfeil (1986).

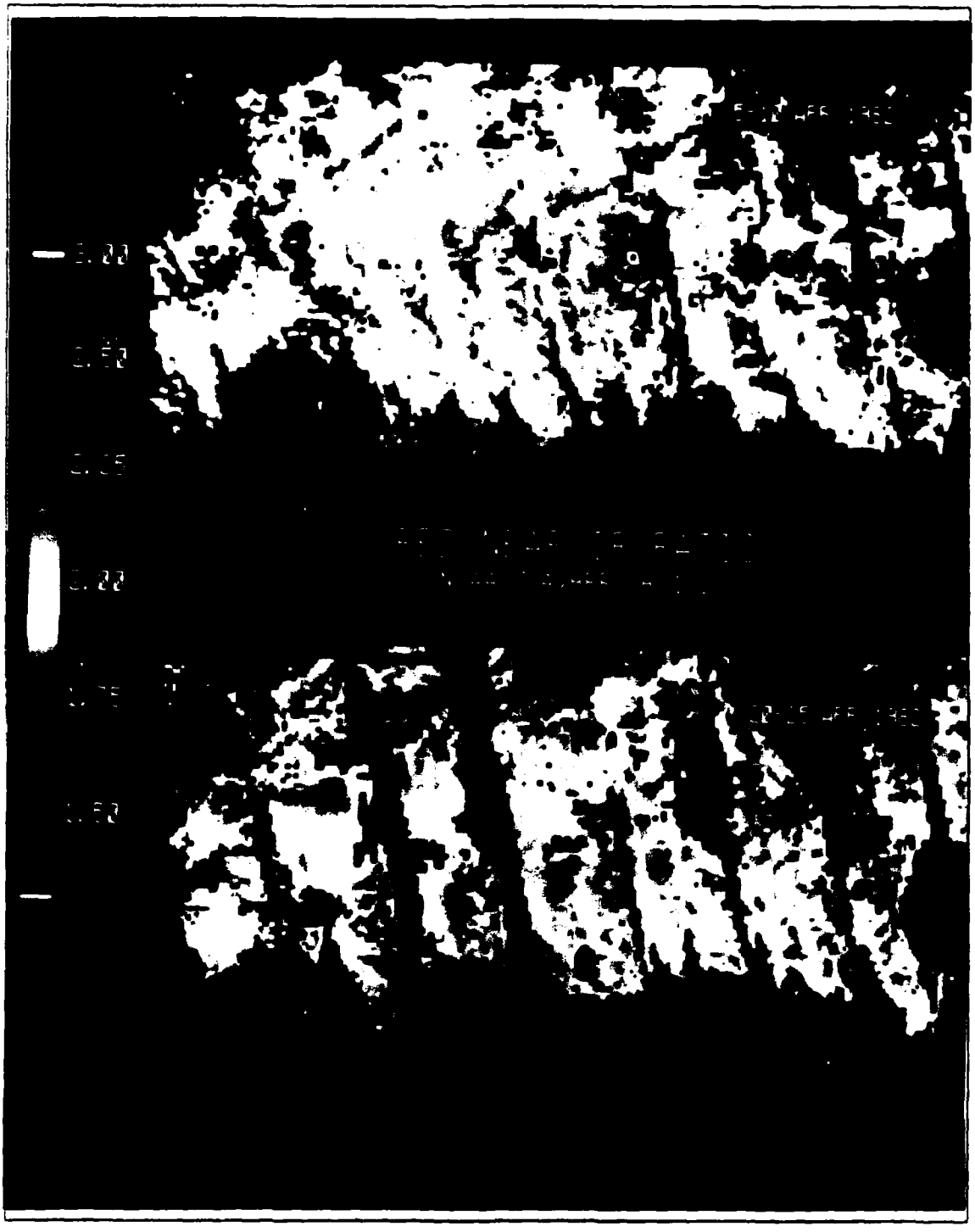

Fig. 8. Aerosol Particle Size Index for early and late April 1982.

2. Albedo and Optical Depth

Pfeil (1986) did not estimate optical depth. Instead albedo was used to estimate atmospheric conditions. It is much better to use optical depth, which gives an understanding of the transmittance capabilities of the entire atmospheric layer, rather than albedo which measures the total amount of radiance reflected back to the satellite. From Fig. 9, which reproduces Pfeil's albedo results, it is easy to see that albedo is affected by the sun-satellite view geometry. This may be due to the effects of Rayleigh radiance, which was discussed above in connection with albedo ratios.

Fig. 10 shows the optical depths obtained using the present method. In this figure, a high optical depth region extends west into the North Pacific Ocean from Central America. There is a similar feature in Fig. 9. However, in Fig. 10 the feature is a continuous discrete band that has the appearence of being a natural occurrence, while the feature observed in Fig. 9 is very disjointed and looks as if it may be an artifact of the processing. The optical depth values, although high, are consistently in the 0.3 to 0.4 range, without many discrete breaks. The albedo starts at 12% and decreases to 2%, then jumps back to 12% as the feature is tracked westward. There is a similarly occurring feature in the later half of April 1982 in the western North Pacific that shows the same differences as those just described for the eastern North Pacific.

Cloud contamination appears to be more evident in albedo than optical depth. In the albedo results, high values were located in all areas normally associated with large cloud coverage. In particular, cloud contamination is the cause of high albedos in the region of the South Pacific Convergence Zone. In the same region, the optical depths were all low. While this area is a cloudy region, the cloud discrimination removed all the cloudy pixels when computing optical depth, while the albedo technique did not perform as well.

3. Aerosol Particle Size Index and Optical Depth

Analyses were performed intercomparing early April 1982, late April 1982 and April 1983. As discussed in Chapter II, these time periods were not identical. The early and late April 1982 data comprised two separate six-day periods, while the April 1983 data consisted of the 15 odd numbered days, covering the full month. Additionally, the 1982 data were primarily in the North and South Pacific and the 1983 data was global. However, these differences did not pose any difficult problems in the analysis.

In April 1982 the dominant synoptic pattern was the slow development of a strong long wave ridge in the mid North Pacific Ocean, with a long wave trough axis over eastern China. Early in April 1982 the polar jet south of Japan was primarily

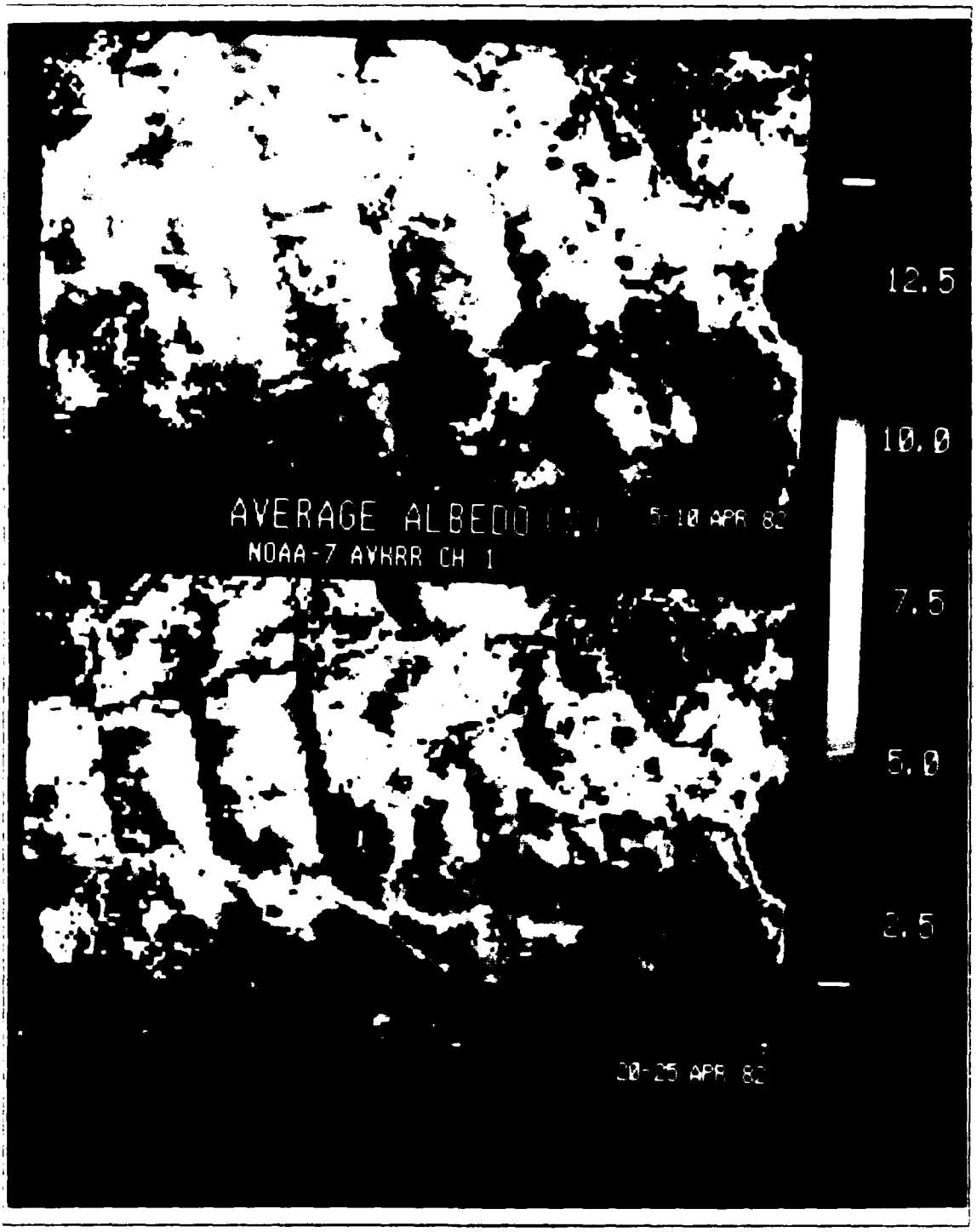

Fig. 9. Albedo for April 1982 from Pfeil (1986).

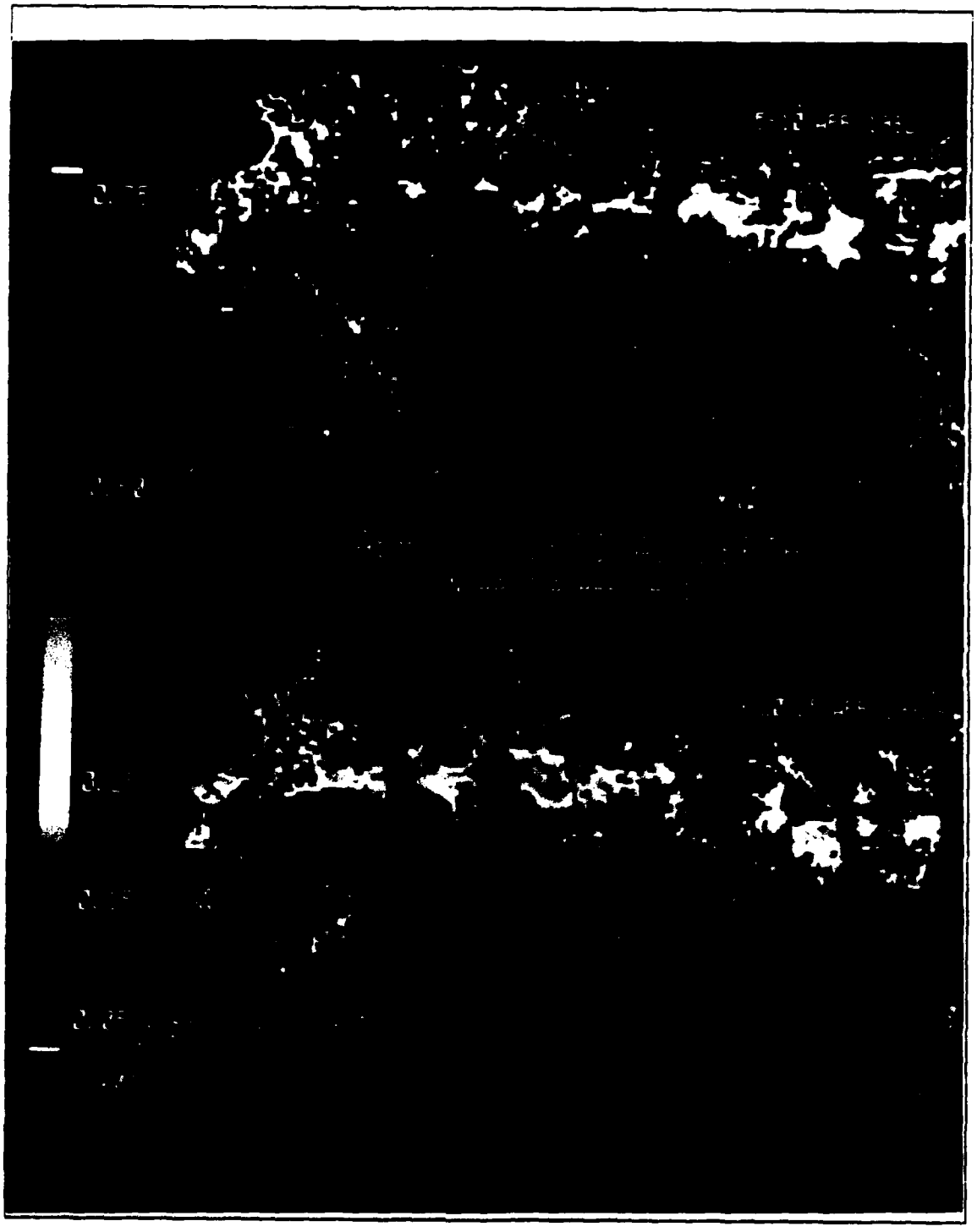

Fig. 10. Optical depth from April 1982.

westerly. With the development of the long wave pattern described above, the jet turned towards the north slightly, as southwesterly flow. At the same time, strong cyclonic activity, associated with the long wave trough, over the Gobi desert was causing strong dust storms. These conditions resulted in favorable conditions for long range dust particle transport over the North Pacific.

The major aerosol particle producing event, for 1982, was the eruption of the El Chicon volcano (17.3°N, 95.2°W). There were several eruptions between 28 March and 6 April 1982. Debris from these eruptions moved both west and east (Krueger, 1983). This would produce some significant effects upon the optical depths and the S_{12} values.

A basic overall pattern in optical depth estimates is that there are lower values in the southern hemisphere compared to the northern hemisphere. A typical value in the southern hemisphere is 0.1 or less, while in the northern hemisphere, optical depth is consistently 0.15 or greater. This is shown in Fig. 10, April 1982 optical depth estimates, and in Fig. 11, which presents the April 1983 optical depth estimates. This optical depth pattern is a result of the greater land mass located in the northern hemisphere. Land-derived aerosol particles are in a much larger quantity in the northern hemisphere, both naturally occurring and man-made, which results in the larger optical depth estimates in the northern hemisphere.

In early April 1982 (Fig. 10) there is a maxima greater than 0.25, found off the west coast of Mexico that and extending west about one third of the way across the North Pacific Ocean. Other maxima of similar values are located along most of the eastern Asian coast line in early April, along with a few isolated areas in the mid North Pacific. In the Gulf of Mexico there is a realtively high maxima (almost 0.5) that extends north and east.

In the later half of April 1982 many of the same maxima exist, with one major exception. The maxima off the coast of China in the East China Sea extends far to the east and has increased in thickness in some locations to 0.6 or greater. It appears to be merging into the maxima from the west that is still evident.

The high optical depths just noted are, with a few exceptions, all in areas which are adjacent to large land masses. Two of these maxima, along the East China Sea and the southern Mexican coast, are located near major aerosol particle producing events. Gobi desert dust and El Chicon debris would be expected to produce high optical depths.

April 1983 shows evidence of dramatic changes in optical depth from the previous year. The strong maxima that extended across the North Pacific Ocean is no longer

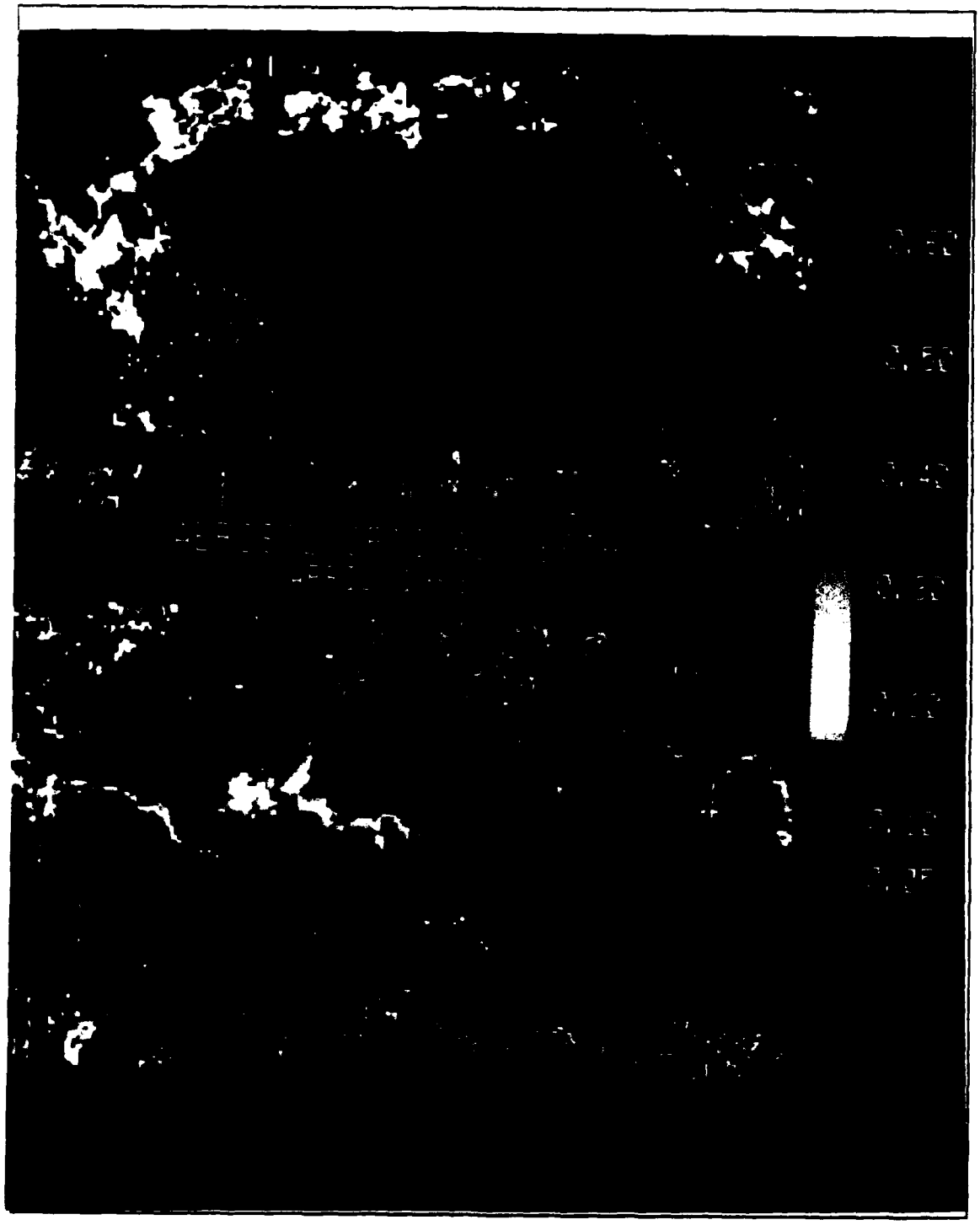

Fig. 11. Optical depth from April 1983.

present, although there is a very small area that has very high values of optical depth, greater than 0.25, along the western coast of Central America. There are also high values observable, again, in the East China Sea and there is a region of high optical depths surrounding the island of Borneo. These results are consistent with the 1982 results. In 1983, El Chicon was not erupting, so optical depths would be expected to be lower in that region. The maximum near Borneo coincides with one of the worst series of bush fires ever recorded in that part of the world (Voice and Gauntlett, 1984).

Elsewhere around the globe in the 1983, there is a very high maxima extending out of western Africa into the North Atlantic, with thickness values exceeding 0.5 close to the coast. There are also maxima greater than 0.25 in the Amazon delta basin, the Gulf Coast of the United States and near dense coastal population centers. The optical depths also appear to be reasonable over smaller bodies of water, which was not expected.

In April 1982 the dominant S_{12} feature is high values, above 2.5, in the tropical North Pacific Ocean (Fig. 8). The values were higher in the eastern ocean averaging 2.4, with a decrease westward to an average of 2.2. As noted above, the S_{12} values decreased poleward, with a greater decrease in the southern hemisphere vice the northern hemisphere.

Also, in early April 1982, there is a maximum S_{12}, greater than 2.5, along the northern coast of Australia which is not observed later in the month. There is also a secondary diffuse S_{12} maximum, aproximately 2.25, spread over a large portion of the Philippine Sea in the early part of the month. This changes dramatically in the second half of the month, when a strong S_{12}, ranging from 2.25 to 2.50, comes off the southern coast of China, extends through the East China Sea and east into the Philippine Sea before curving to the northeast in to the mid north Pacific Ocean. Other S_{12} maxima that are observed in both early and late April 1982 are along densely populated coastal areas, such as the Chinese coastline, around Japan and the west coast of the United States.

Just barely visible along the eastern edge of Fig. 8 is the Gulf of Mexico and the Caribbean. Careful note should be made of the very high S_{12} located to the south of Florida, as well as the one found along the Gulf Coast of the United States.

April 1983 (Fig. 12) shows a dramatic change in the overall S_{12} pattern observed in 1982. The tropical maximum that extends across the North Pacific is dramatically diminished. Where S_{12} values were 2.0 or greater in 1982, they almost never exceeded 2.0 in 1983, and were often much less than that. The strong maxima found along the

west coast of northern South America is just barely visible and is much weaker. Along the coast of the western United States and Mexico the values are greatly diminished with the exception of isolated maxima near Los Angeles and San Francisco, which retain S_{12} values greater than 2.5.

The pattern of decreasing S_{12} values poleward, with a greater decrease in the southern hemisphere, continues in April 1983. Since 1983 is a global scale analysis, this pattern is observed throughout the entire globe as can be seen in Fig. 12

The maxima south of Florida noted in the 1982 analysis appears again in 1983. Again, it is one of the highest S_{12} maxima found around the globe, maintaining a value in excess of 3.0. Maxima along the Gulf Coast of the United States are still visible as well as coastal maxima along the Chinese and Japanese coastlines. Elsewhere around the globe, maxima are found in coastal regions near dense population centers, such as Bombay and Calcuta as well as in some areas of high industrial output, like the oil refinery areas of the Persian Gulf. One interesting region of high S_{12} values is the broad delta region of the Amazon river.

Due to the nature of requiring clear air in a low optical depth region, it was expected that this procedure would only work over oceanic regions. However, maxima are clearly visible in the Great Lakes region near Detroit, Chicago and Clevland. Results are also obtainable in other small bodies of water, such as the Mediterranean, Black and Caspian seas.

The S_{12} results can, in many cases be correlated to the optical depth results. High S_{12} values were often located in proximity to land masses and naturally occurring events. However, some high values were observed in regions far removed from land sources, without any apparent means of reaching those remote areas. These will be discussed in more detail below.

At this point it should be remembered that the S_{12} value is the slope of the aerosol size distribution curve. It does not provide any absolute value as to the number of various sized aerosol particles present. The slope may remain the same for a large number of aerosol particles as a small number of aerosol particles. What it does reveal is the relative size of the dominant aerosol particle. High values denote small aerosol particles (submicron) and low values denote large aerosol particles (supermicron). Therefore high S_{12} values indicate that small aerosol particles dominate, but there is no evidence for the number of aerosol pariticles present.

In several areas, high S_{12} values are collocated with high optical depths. This is seen in the eastern North Pacific along the coasts of Mexico and the United States as

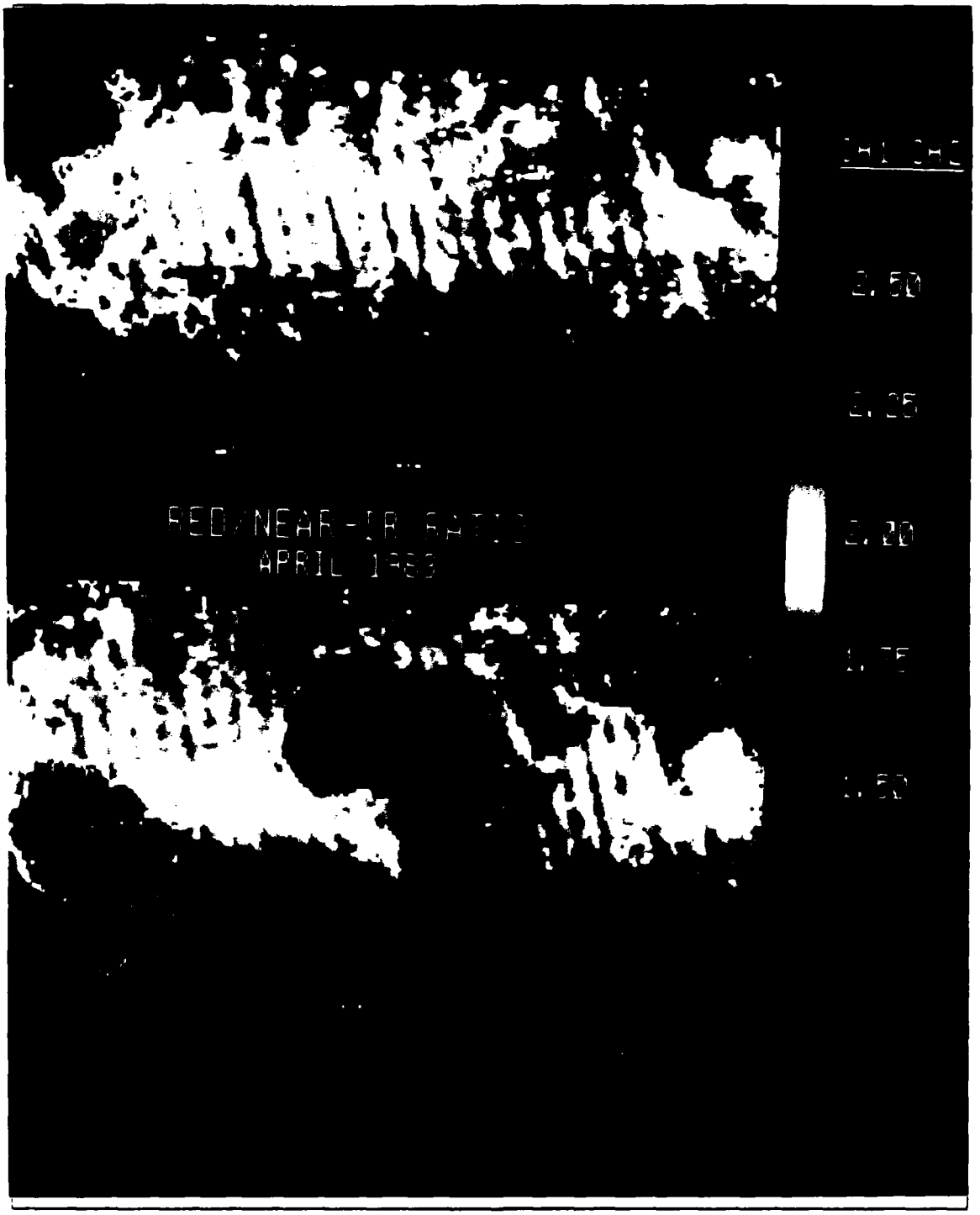

Fig. 12. Aerosol Particle Size Index, April 1983.

well as along the eastern Asian coast line. This would indicate that there is a very high number of aerosol particles in the atmosphere, hence the thick optical depth values. Since the transmittance of the atmosphere decreases as optical depth increases, high optical depths are indicative of some scaterring or absorbtive agents. The high S_{12} values in the same regions show that the distribution of the aerosol particles are weighted towards smaller particles. Therefore, it is reasonable to conclude that large amounts of aerosols, continental in origin, are blowing off the land and out over water in these areas. They do not extend great distances, because they tend to settle out before they have a chance to travel extensively. The particles that settle out are also large enough to form CCN. As such, they will also settle from rainout.

The maximum in the ratio extending out into the North Pacific Ocean from the El Chicon region is also collocated with a very high optical depth value. This extension into the North Pacific is from strong low and mid level easterlies carrying the volcanic debris out over the ocean. Note however, that the extent of the high optical depths is not as great as the S_{12} values. This is most likely due to the settleing of the low level debris out of the atmosphere as it moves away from the volcano.

Krueger (1983) showed that the debris from El Chicon moved east in addition to moving west. He proposed that this eastward movement was from debris that had been ejected up into the stratosphere. High optical depths are observed extending north and then to the east of El Chicon in early April 1982. They are not evident in late April to the extent that they are in the earlier portion of the month. An analysis of the the upper-level winds, Fig. 13, shows southerly flow over the El Chicon region, which then turns into westerly flow further north. This appears to support the contention of Krueger (1983) that some of the debris blew to the east.

In the western North Pacific, the high optical depths are in the same regions along the coastlines as the high S_{12} values in the early part of April 1982. Then, in the second part of the month they both extend out into the North Pacific. Earlier, in the middle of the month, several strong cyclones swept through the Gobi desert. It is not uncommon for the dust from the Gobi desert to blow long distances out over the ocean (Shaw, 1980). The high S_{12} values in late April follow the mid- and upper-tropospheric wind patterns given by Fig. 14. Therefore these high S_{12} values are probably from dust originating in the Gobi desert. Notice, again, how the optical depths decrease with the distance from land. This also provides evidence that the source of the aerosol particles producing the high S_{12} values are settling out of the atmosphere as they travel.

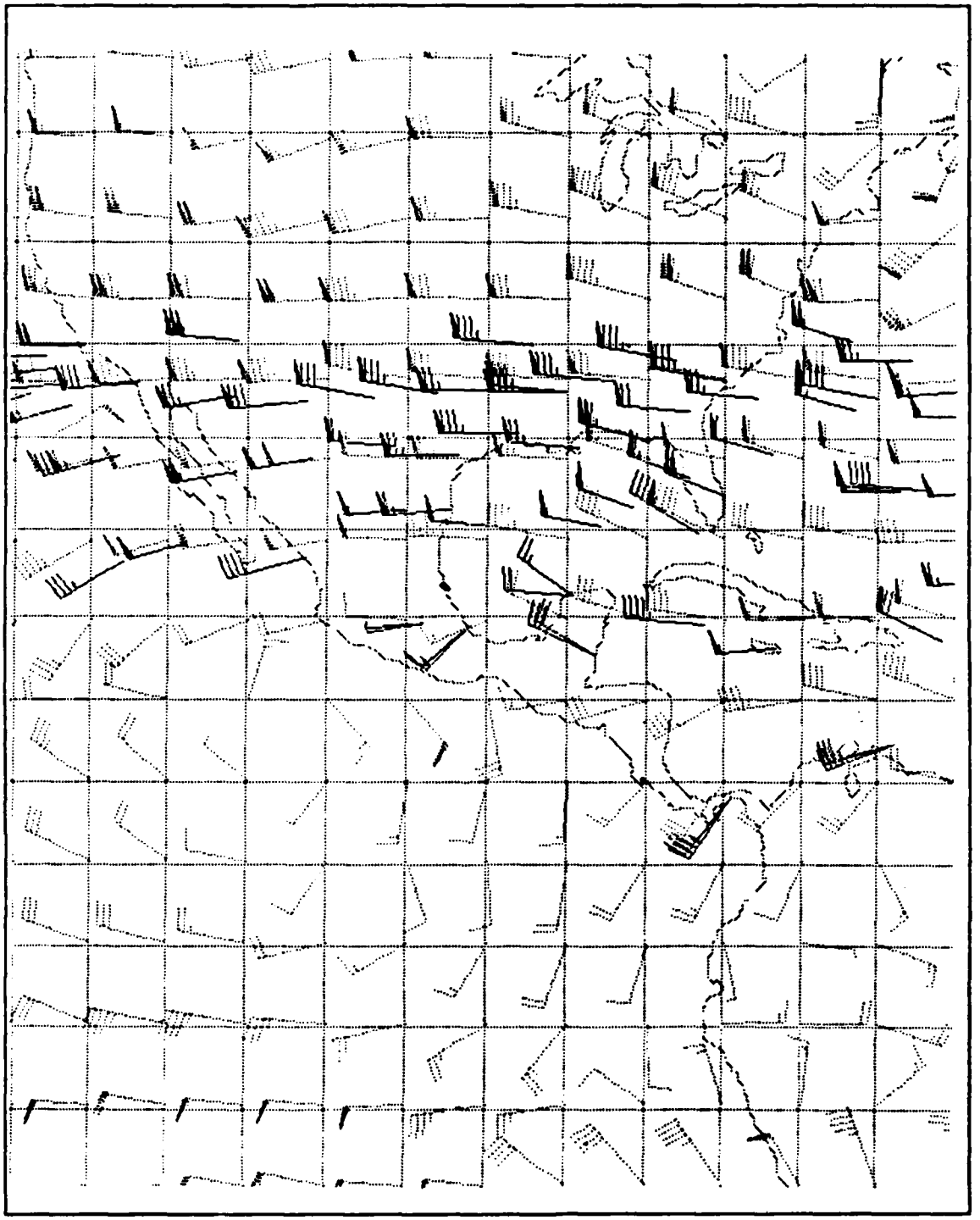

Fig. 13. 250 mb Global Band Winds, 5 April 1982.

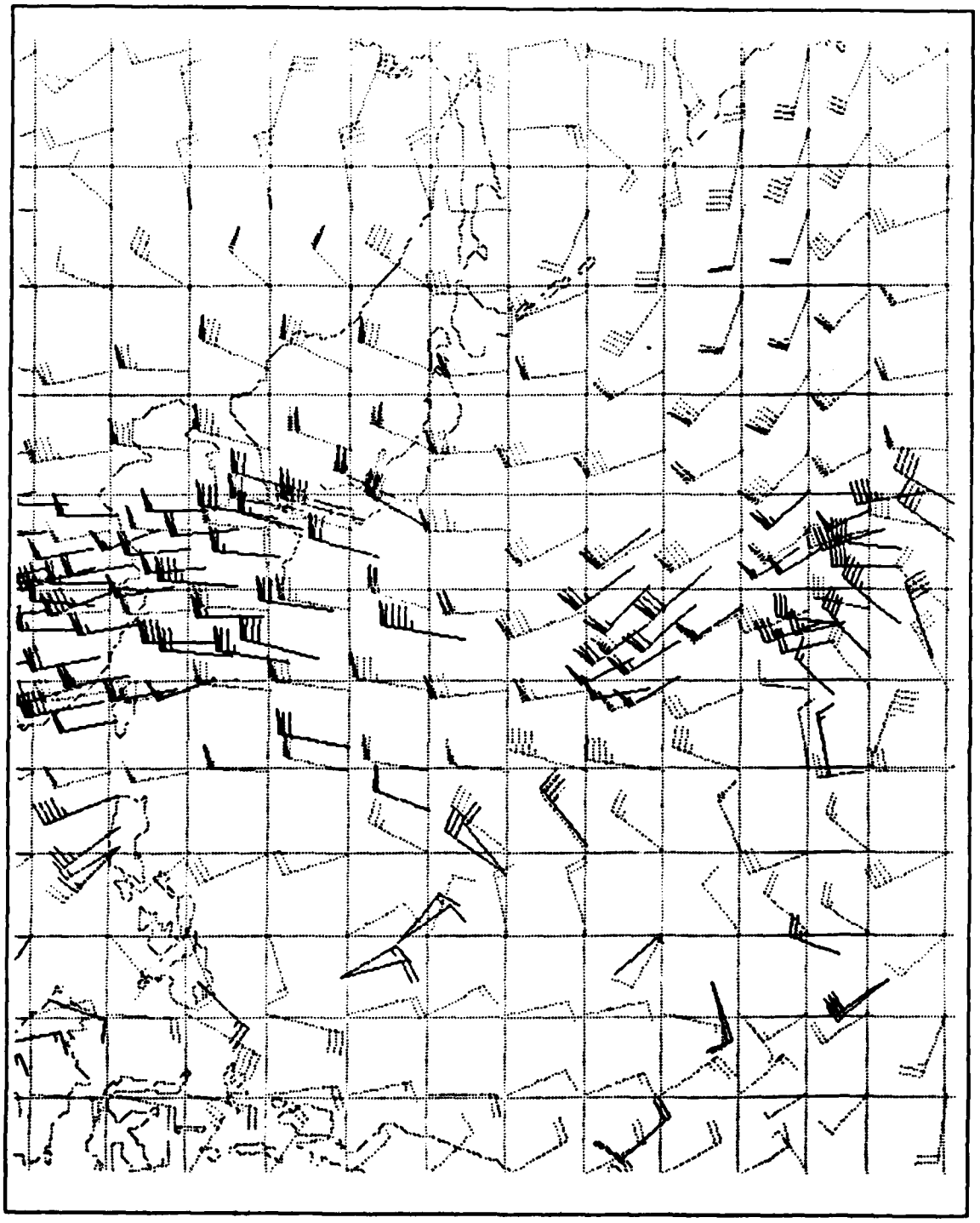

Fig. 14. 250 mb Global Band Winds, 20 April 1982

Evidence of blowoff from Asia, most likely Gobi desert dust, was also seen in April 1983. High S_{12} values were all along the coast, with decreasing values further east out over the ocean. Higher optical depths were also noted along with these higher S_{12} values. The extent of this blowoff was not as great or as strong as the 1982 event. This may be due to weaker winds over the interior portion of the Asian continent in April 1983 versus April 1982.

Pfeil (1986) did an extensive analysis of the high S_{12} values found along the northern coasts of Australia. While his results covered a much larger area, particularly off the northwestern coast Australia in the latter half of April 1982, they were still in a similar range as the present study. He proposed that strong offshore flow accounted for the increased S_{12} values over water. However, the optical depths, which he did not evaluate, show very low thickness values in this region, with a small exception in the Gulf of Carpentaria and south of Port Moresby. This means that there may be aerosols blowing off the coast of Australia, however, they must all be small and in a much lower concentration then seen in the Gobi desert dust or the El Chicon debris. Therefore, north of Australia, small aerosol particles dominate, but there are less aerosol particles overall than in the two cases discussed above.

The tropical region extending across the North Pacific is similar to the areas north of Australia, in that there are high S_{12} values but low optical depths. This area had very high S_{12} values in the east, that slowly decreased westward. There is no similar trend with regards to the optical depths. This denotes that there are very high levels of small particles compared to large particles. However, the overall number of particles must be reduced compared to the Gobi dust and El Chicon debris. Pfiel (1986) had this same feature in his results and hypothesized that the convergence of equatorial easterlies might account for this maximum, with a continental derivation of aerosol particles. However, up to this point, the cases that have been observed containing continentally derived aerosol particles long distances from the coast start with very thick optical depths along the coastline. This is not evidenced in this case. Also, the line of maximum values is to the south of the April ITCZ. There must be some other source, most likely an oceanic source.

Andrea (1985) found that dimethylsulfide (DMS) concentrations are very high in upwelled tropical waters. Clarke (1987) found an increase in atmospheric sulfur compounds in the equatorial regions. In particular he found very high elevations of small sulfur based aerosol particles all along the equatorial upwelling regions. Given that coccolithophorids are prime producers of DMS (Andrea and Raemdonck, 1983) and

that the dominant phytoplankton in equatorial regions are coccolithophorids (Hasle, 1959; Okada and Honjo, 1973), then it is conceivable that the high S_{12} values in the equatorial regions are from a flux of biogenic sulfur across the air sea interface with a subsequent conversion to sulphate particles as hypothesised by Charlson et al. (1987).

The first observation concerning the overall pattern in April 1983 is the lower values for the aerosol particle size index in the tropics. If as surmised above, that the equatorial maxima are due to marine biogenic sulfur compounds, then this reduction might be expected. The time period, April 1983, was during the 1982-1983 El Nino-Southern Oscillation event. Starting in October 1982, upwelled ecosystems in the eastern equatorial Pacific began a transition from normally high productivity to low productivity that did not return until July 1983 (Barber and Chavez, 1983). Feldman et al. (1984) found a complete change from the normal phytoplankton distribution by March 1983 in the eastern equatorial Pacific Ocean. This tends to support the hypothesis of Charlson et al. (1987) that phytoplankton are responsible for a large portion of marine aerosol particles.

Outside of the North and South Pacific Oceans, the most noticeable feature in April 1983 was the high optical depths observed extending from the west African coast into the North and South Atlantic. This is consistent with observations confirming Saharan dust from the coast of Africa extending into the western Atlantic basin and into the Caribbean (Prospero, 1982).

The other interesting feature is the high S_{12} values and thick optical depths found along the Amazon river delta. This region is known to be one of the most highly productive biological regions in the world. Lovelock et al (1972) discussed the production of aerosols from terrestrial forests as a biological emission. This may possibly account for some of this increase. A second possibilty is the clearing of land in the tropical rain forest through large scale burning. This would also introduce large amounts of aerosol particles into the atmosphere. This is most likely the cause of the high values observed on either coast of Central America in April 1983.

The most consistent area of high S_{12} value is the location south of Florida that has these values both in 1982 and 1983. The consistency in position and strength is extrordinary. While there are several tropical islands that may provide a contamination from land into the process, this is not observed in other areas, such as the Hawaiian Islands. In fact the process for determining S_{12} values should produce lower values over land, which is evidenced in Fig. 8 and Fig. 12. These islands do not contain dense population levels nor do they have the heavy industry they may account for these values.

Neither are the waters surrounding the islands anywhere near as productive as the equatorial upwelled regions. Thus this region remains an anomalous region that requires more study.

B. CLEAR PIXEL POINTS

The number of clear pixel points was recorded in order to determine the statistical relevance of the data set. Additionally, the converse of the clear pixel points would provide a indication of the cloud representation during the month. In Fig. 15 and Fig. 16, which show the pixel counts for April 1982 and 1983, respectively, there is a maximum in clear pixel points in the tropics, with 1983 shifted slightly northward of the 1982 position.

As can be seen from Fig. 15 and Fig. 16 there is consistently more than 500 pixel points in most of the 1° by 1° boxes in the images. This means that the averaging technique used over 500 data points for each S_{12} value and optical depth estimate. In many cases the number of data points exceeded 1,000 points.

One thing that can be noticed is that the number of points appears to increase in the center of the passes. This is due to the overlapping nature of the passes and the removal of pixel points through sun glint removal or the elimination of pixels from the edges because of reduced resolution (16 pixels from each edge of a pass).

In the tropical area of very high S_{12} values during April 1982, there is a corresponding high number of clear pixel points. This would seem to indicate that these very high S_{12} values, with low optical depths, do not produce a significant amount of clouds. Just to the north of this high S_{12} area is the ITCZ. Notice that the S_{12} values decrease as well as the number of clear pixels. The easterly winds that converge at the ITCZ can move these small aerosols, which will be undergoing nucleation and hydroscopic growth with time, into that ITZC. By the time they reach the ITCZ, they will be large enough to form cloud condensation nuclei. Hoppel et al. (1987) demonstrated how DMS, the sulfur compound that may be the cause of these aerosol particles, can undergo the neccessary chemical and physical growth processes in order to reach cloud condensation nuclei size. This also provides more evidence that the tropical aerosol particles may be biogenic.

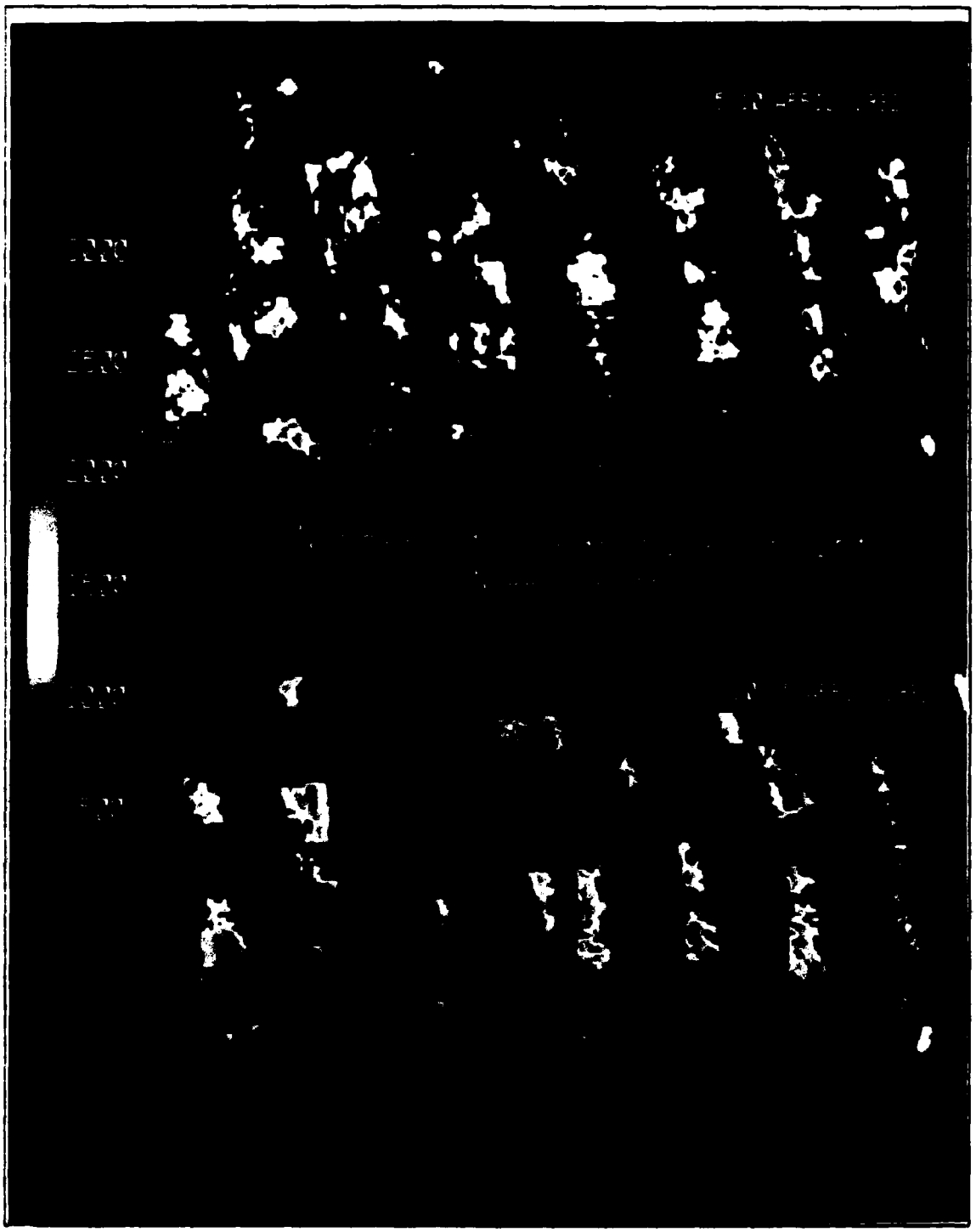

Fig. 15. Number of clear pixels used for April 1982.

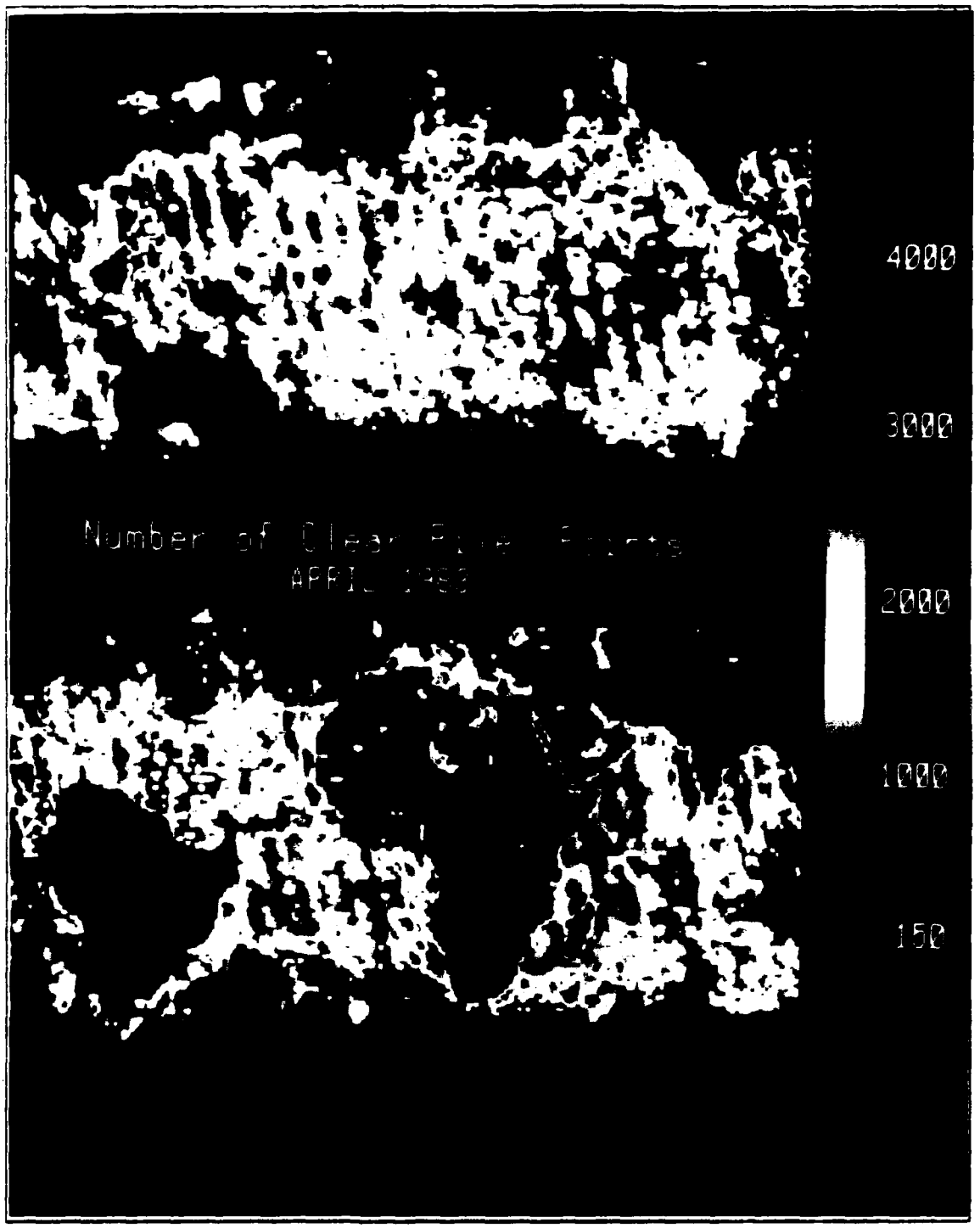

Fig. 16. Number of clear pixels used for April 1983.

V. CONCLUSIONS AND RECOMMENDATIONS

Several conclusions can be drawn from the results discussed above. These can be split into two major sections. The first section deals with the technique and it's improvements. The second focuses on the results of a satellite-derived global analysis of optical depth and Aerosol Part Particle Size Index (S_{12}).

It is obvious from the results that the improved techniques produced some significant results. Foremost among these was the introduction of a variable phase function. Without the variable phase function, it would not have been possible to perform a global scale averaging of optical depth. All the previous work estimating optical depth indicated that, while varying the phase function was desirable, it was considered too difficult to implement. This work showed that not only was it essential to vary the phase function, but that it could be done.

The cloud discrimination technique performed much better than the earlier technique. Evidence from this improvement is the reduction in cloud contamination that was contained in the earlier results. This also permited a method of discriminating between clouds and aerosols that was not available earlier.

The sunglint removal improvement added additional data that was previously lost to processing. The removal of Rayleigh radiance and the accounting for ozone absorption produced a more accurate aerosol particle size index. The estimation of optical depth vice albedo gives a better understanding of the radiative transfer characteristics of the atmosphere. It also allowed for a correlation between optical depth and APSI values which was very useful in identifying the type of aerosol particles.

The data processed provided several interesting results. A spatial view of the relative aerosol size distribution was possible from the APSI values. It was easy to distinguish man-made increases over naturally-occuring increases. More evidence was provided that showed the ability of the atmosphere to transport aerosol particles great distances, both in the North and South Atlantic Ocean as well as in the North and South Pacific Ocean.

Some evidence was provided for the theory that much of the aerosol particle population, at least in the tropics, is biogenic in origin, and that there may be a biological feedback mechanism in the earth's radiation budget. This evidence was provided through intercomparing data during an El Nino-Southern Oscillation time period with one that came before it. The drastic change, particularly in the eastern North Pacific

Ocean, showed that there is some form of climatic influence on aerosol particles in the tropics.

The evidence would have been more substantial if more data could have been processed. This may be in the form of continuing to process only April data for a number of years and or processing a years worth of data prior to, during and after the El Nino-Southern Oscillation event. If the values remain consistent before and after the El Nino-Southern Oscillation event and show a decline during the event, this would provide more proof of biogenic origins. Additionally, it would be advantageous to have cruise data that included aerosol particle collections as well as phytoplankton measurements. That, in addition to the satellite data, should be able to prove or disprove this theory.

One improvement in the technique that should be implemented in the future would be to obtain the APSI from optical depth ratios vice radiance ratios. This should eliminate the slight geometric bias that is observable in Fig. 12. Since the geometric bias has been eliminated from the optical depth and the radiance ratio is an approximation for the optical depth ratio, it would be better to calculate this directly. This would also provide a better correlation between optical depth and APSI values.

This study presents an excellent tool for the evaluation of aerosol particles on a global scale. With a few minor modifications, it hopefully will provide critical data for long term global radiation studies.

LIST OF REFERENCES

Andrea, M. O., 1985: Dimethylsulfide in the water column and sediment pore waters of the Peru upwelling area. *Limnol. Oceanogr.* , **30(6)** , 1208-1218.

Andrea, M. O. and H. Raemdonck, 1983: Dimetylsulfide in the surface ocean and the marine atmosphere. *Science*, **221**, 744-747.

Barber, R. T. and F. P. Chavez, 1983: Biological consequences of El Nino. *Science*, **222**, 1203-1210.

Bullfinch, S. R., 1986: Determination of the atmospheric aerosol distribution by multi-channel remote sensing techniques. M.S. Thesis, Naval Post Graduate School, Monterey, CA, 87pp.

Carlson, T. N., 1978: Atmospheric turbidity in Saharan dust outbreaks as determined by analysis of brightness data. *Mon. Wea. Rev.* , **237** , 452-453.

Carlson, T. N., and J. M. Prospero, 1972: The large-scale movement of Saharan air outbreak over the North Equatorial Atlantic. *J. Appl. Meteorol.* , **11** , 283-291.

Charlson, R. J., J. E. Lovelock, M .O. Andrea, 1987: Oceanic phytoplankton, atmospheric sulfur, cloud albedo and climate. *Nature*, **326**, 655-661.

Charlson ,R. J. and M. J. Pilat, 1969: Climate: The influence of aerosols. *J. Appl. Meteor.* , **8**, 1001-1001.

Chylek, J. E. and J. A. Coakley, 1974: Aerosols and climatology. *Science*, **183**, 75-77.

Clarke, A. D., 1987: The Pacific marine aerosol: evidence for natural acid sulfates.*J. Geophys. Res.*, **92 (D4)**, 4179-4190.

Coakley, J. A. 1976: Aerosols and the Earth's radiation budget. *Radiation in the Atmosphere*. H. J. Bolle, ed., Science Press, Princeton, NJ, 472-474.

Durkee, P. A., 1984: The relationship between marine aerosol particles and satellite-detected radiance. Ph.D. Thesis, Colorado State University, Fort Collins, CO, US ISSN 0067-0340, 124 pp.

Durkee P. A., D .R. Jensen, E. E. Hindman and T .H. Vonder Haar, 1986: The relationship between marine aerosols and satellite detected radiance. *J. Geophys. Res.*, **91(D4)**, 4063-4072.

Feldman, G., D. Clark and D. Halpern, 1984: Satellite color observations of the phytoplankton distribution in the eastern equatorial Pacific during the 1982-1983 El Nino. *Science*, **226**, 1069-1071.

Fleagle, R. W. and J. A. Businger, 1980: *An Introduction to Atmospheric Physics* , Academic Press, New York, NY, 432 pp.

Hasle, G. R., 1959: A quantitative study of phytoplankton from the equatorial Pacific. *Deep Sea Res.*, **6**, 38-59.

Hoppel, W. A., J. W. Fitzgerald, G. M. Frick, R. E. Larson and B. J. Wattle, 1987: Preliminary investigation of the role that DMS and cloud cycles play in the formation of the aerosol size distribution. NRL Report 9032, Naval Research Laboratory, Washington, DC, 33 pp.

Jensen, J. R.,1986: *Introductory Digital Image Processing; A Remote Sensing Approach.* Prentice-Hall, Englewood Cliffs, NJ, 379 pp.

Kellog, W. W., R. D. Cadle, E. R. Allen, A. L. Lazrus and E A. Martell, 1972: The sulfur cycle. *Science*, **175**, 587-595.

Krueger, A.J., 1983: Sighting of El Chicon sulfur dioxide clouds with the Nimbus 7 Total Ozone Mapping Spectrometer. *Science*, **220**, 1377-1379.

Lenoble, J., 1985: *Radiative Transfer in Scattering and Absorbing Atmosphere: Standard Computional Procedures.* , A. Deepak Pub., Hampton, VA, 300 pp.

Liou, K. N., 1980: *An Introduction to Atmospheric Radiation.*, Academic Press, New York, NY, 392 pp.

Lovelock, J. E., R. J. Magg and R. A. Rasmussen, 1972: Atmospheric dimetylsulfide and the natural sulfur cycle. *Nature*, **237**, 452-453.

McCormick, R. A. and J. H. Ludwig, 1967: Climate modification by aerosols. *Science*, **156**, 1358-1359.

Meinert, D. L. and J. W. Winchester, 1977: Chemical relationships in the North Atlantic marine aerosol. *J. Geophys. Res.*, **82**, 1778-1782.

Okada, H. and S Honjo, 1973: The distribution of oceanic coccolithophorids in the Pacific. *Deep Sea Res.*, **20**, 335-374.

Patterson, E. M., C. S. Kiang, A. C. Delany, A. F. Wartburg, A. C. D. Leslie and B.J. Hurbert, 1980: Global measurements of aerosols in remote continental and marine regions: concentrations, size distribution and optical properties. *J. Geophys. Res.*, **85**, 7361-7376.

Pfiel, F. R., 1986: Developing a physical basis for an aerosol climatology of the Pacific ocean. M.S. Thesis, U.S. Naval Post Graduate School, Monterey, CA, 76 pp.

Prospero, J. M., 1982: Dust from the Sahara. *Natural History* **46**, 55-61.

Prospero, J. M. and R. T. Nees, 1976: Dust concentration in the atmosphere of the equatorial North Atlantic: possible relationship tp Sahalian drought. *Science*, **196**, 1196-1198.

Sellers, W. D., 1965: *Physical Climatology* , University of Chicago Press, Chicago, IL, 452 pp.

Shaw, G. E., 1980: Transport of Asian desert aerosol to the Hawaiian Islands. *J. Appl. Meteor.*, **20**, 1254-1259.

Shettle, E. P. and R. W. Fenn, 1979: Models for the aerosols of the lower atmosphere and the effects of humidity variations on their optical properties. AFGL-TR-79-0214 Air Force Geophysics Laboratories, Hanscom AFB, MA, 77 pp.

Twomey, S. and J. Warner, 1967: Comparison of measurements of cloud droplets and cloud nuclei. *J. Atmos. Sci.*, **24**, 702-703.

Voice, M. E. and F. J. Gauntlett, 1984: The 1983 Ash Wednesday Fires in Australia. *Mon. Wea. Rev.* , **112**, 584-590.

Vonder Haar, T. H., and V. E. Suomi, 1971: Measurements of the earth's radiation budget from satellites during a five-year period. part I: extended time and space means. *J. Atmos. Sci.*, **28**, 305-314.

Weiss, R., R. J. Charlson, A. P. Waggoner, M. B. Baker, D. Covert, D. Thorsell and S. Yuen, 1976: Application of directly measured aerosol radiative properties to climate models. *Radiation in the Atmosphere.* H. J. Bolle, ed., Science Press, Princeton, NJ, 469-471.

Woodcock, A. H., 1952: Atmospheric salt particles and raindrops. *J. Meteorol.*, **9**, 200-212.

Woodcock, A. H., 1953: Salt nuclei in marine air as a function of altitude and wind force. *J. Meteorol.* , **10**, 362-371.

Zaitseva, N. A., 1976: The spatial-temporal variability in long-wave radiation fields at the GATE-74 grounds. *Radiation in the Atmosphere.* H. J. Bolle, ed., Science Press, Princeton, NJ, 530-532.

INITIAL DISTRIBUTION LIST

		No. Copies
1.	Defense Technical Information Center Cameron Station Alexandria, VA 22304-6145	2
2.	Library, Code 0142 Naval Postgraduate School Monterey, CA 93943-5002	2
3.	Chairman (Code 63Rd) Department of Meteorology Naval Postgraduate School Monterey, CA 93943-5000	1
4.	Chairman (Code 68Co) Department of Oceanography Naval Postgraduate School Monterey, CA 93943-5000	1
5.	Professor Philip A. Durkee (Code 63De) Department of Meteorology Naval Postgraduate School Monterey, CA 93943-5000	2
6.	Professor Carlyle H. Wash (Code 63Wx) Department of Meteorology Naval Postgraduate School Monterey, CA 93943-5000	2
7.	Dr. James A. Coakley, Jr. National Center for Atmospheric Research Boulder, CO 80307	1
8.	Lt. Edmond M. Frost, USN 88 York Street Stratford, CT 06497	1
9.	Director Naval Oceanography Division Naval Observatory 34th and Massachusetts Avenue NW Washington, DC 20390	1
10.	Commander Naval Oceanography Command NSTL Station Bay St. Louis, MS 39522	1

11. Commanding Officer — 1
Naval Oceanographic Office
NSTL Station
Bay St. Louis, MS 39522

12. Commanding Officer — 1
Fleet Numerical Oceanography Center
Monterey, CA 93943

13. Commanding Officer — 1
Naval Environmental Prediction Research Facility
Monterey, CA 93943

14. Chairman, Oceanography Department — 1
U. S. Naval Academy
Annapolis, MD 21402

15. Chief of Naval Research — 1
800 North Quincy Street
Arlington, VA 22217

16. Office of Naval Research (Code 420) — 1
Naval Ocean Research and Development Activity
800 North Quincy Street
Arlington, VA 22217